

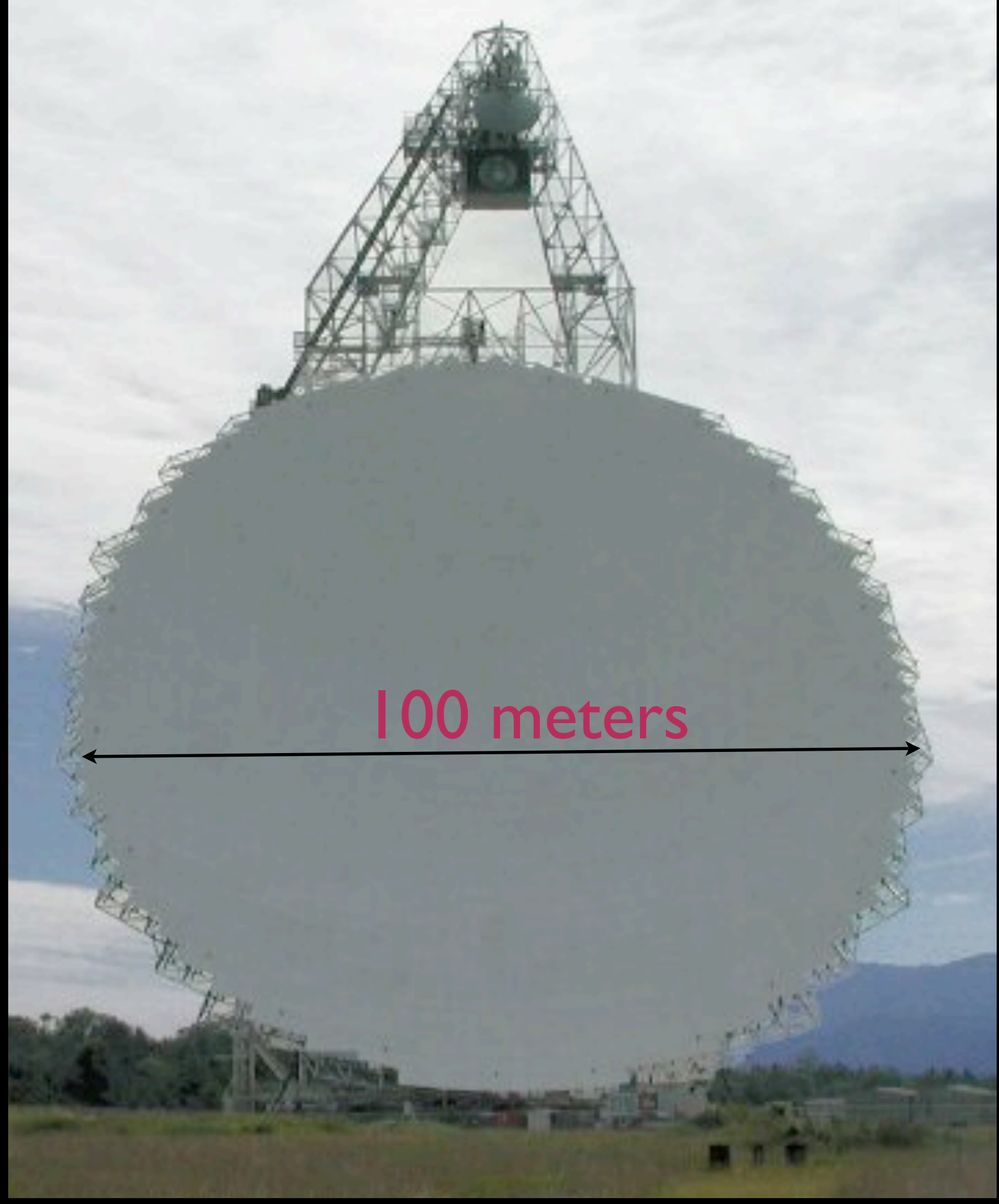
Science Highlights from The Green Bank Telescope



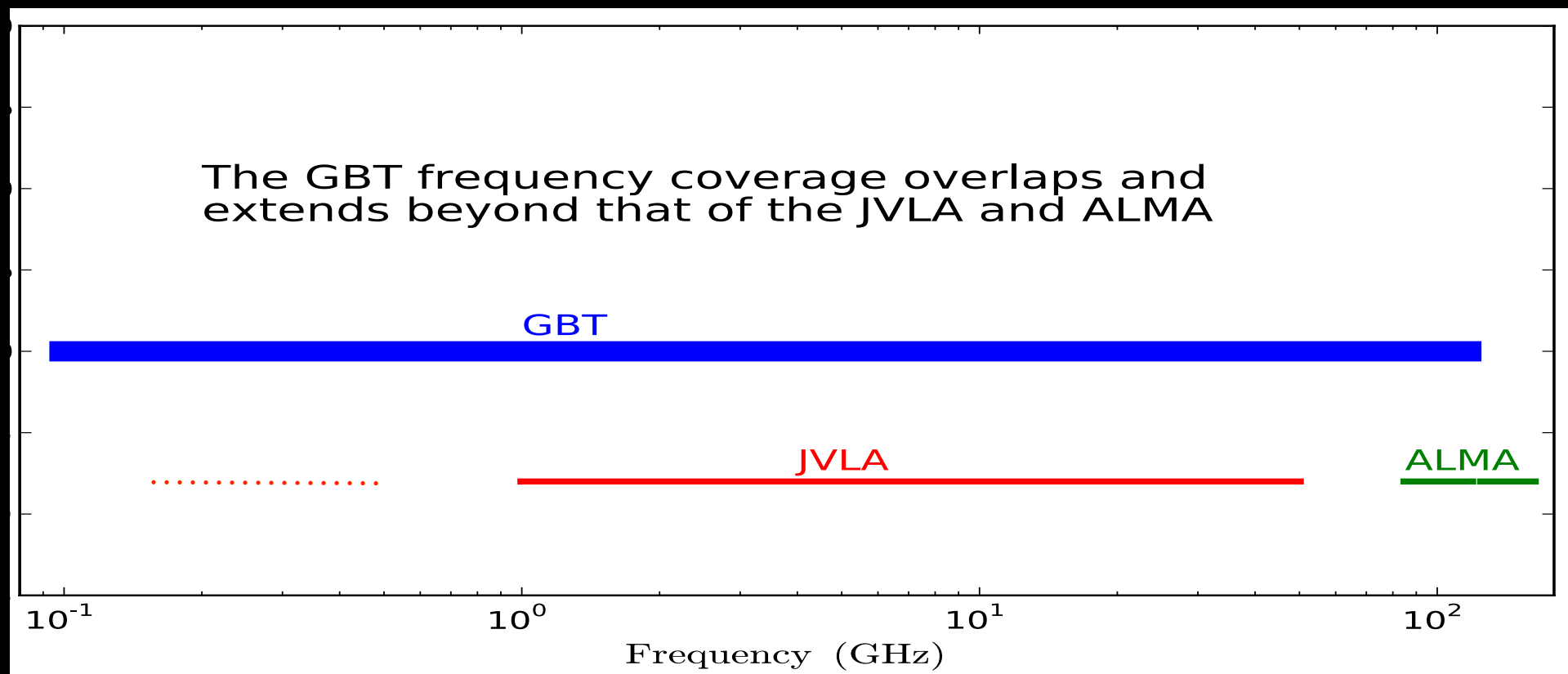
Felix “Jay” Lockman
NRAO, Green Bank WV

The Green Bank Telescope (GBT)

Sensitivity
Radio Quiet Zone



- Receivers cover 0.1 to 100 GHz
- >85% of total sky covered $\delta \geq -46^\circ$
- National Radio Quiet Zone
- Competitively Scheduled



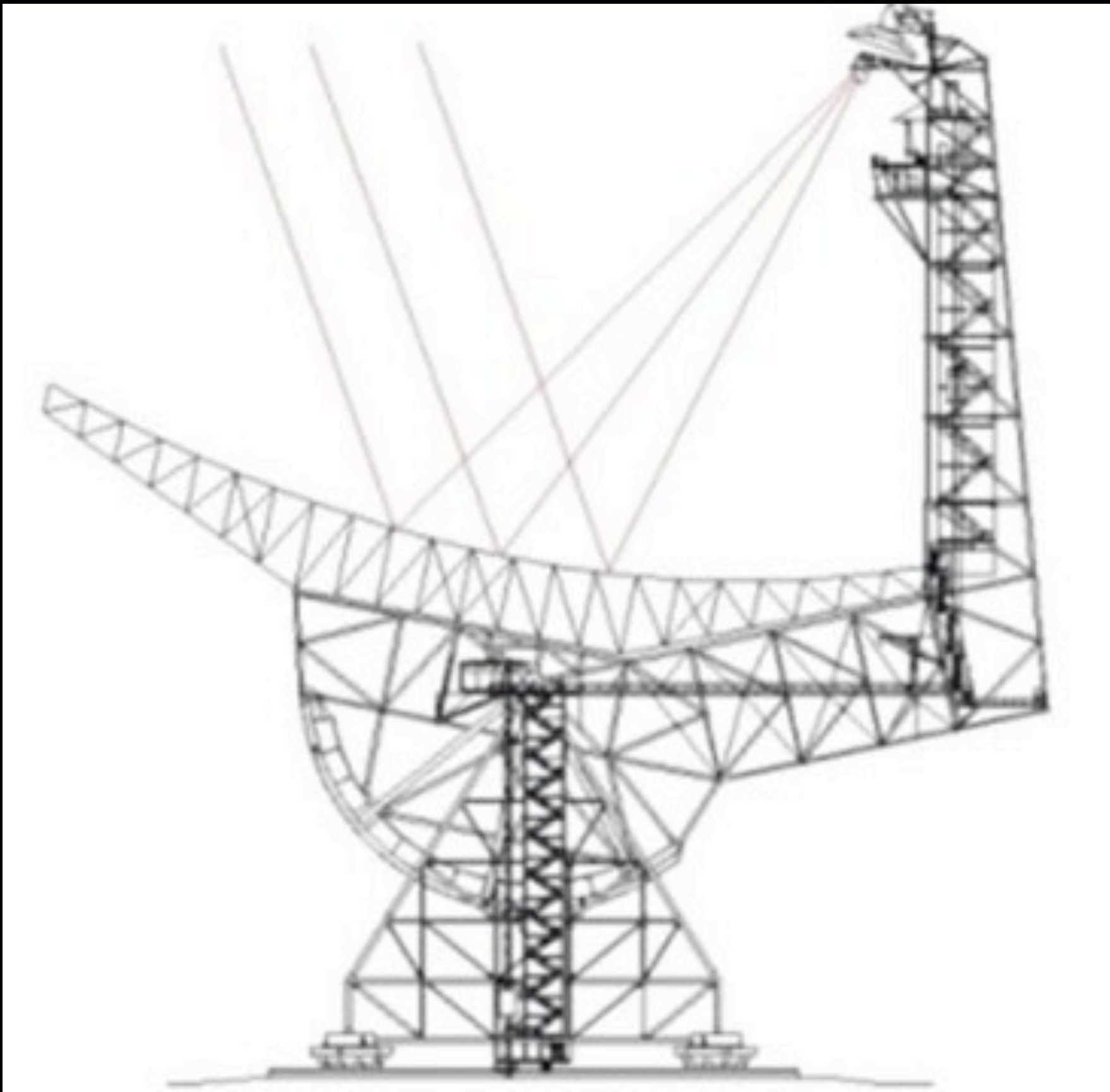
National
Radio
Quiet
Zone

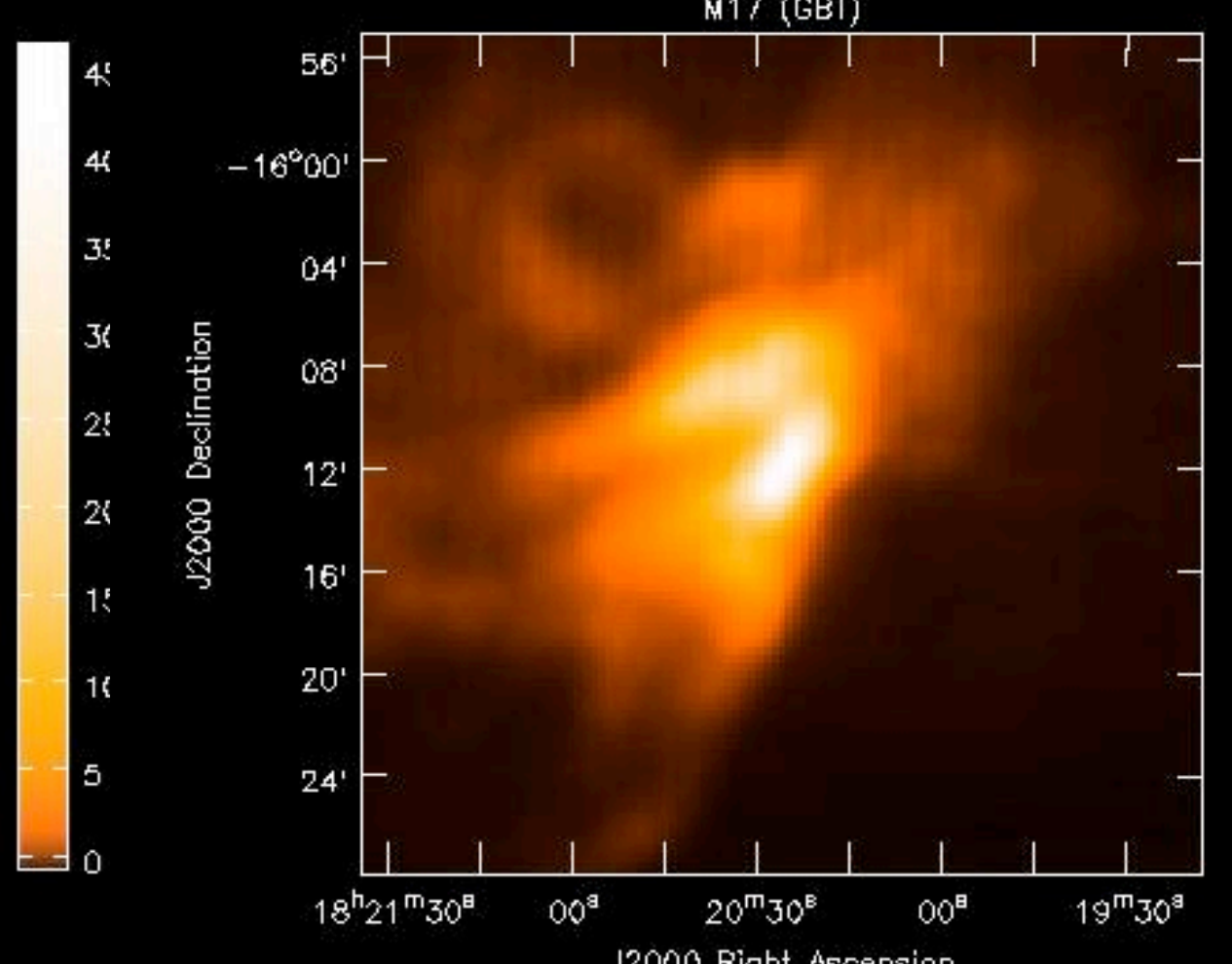
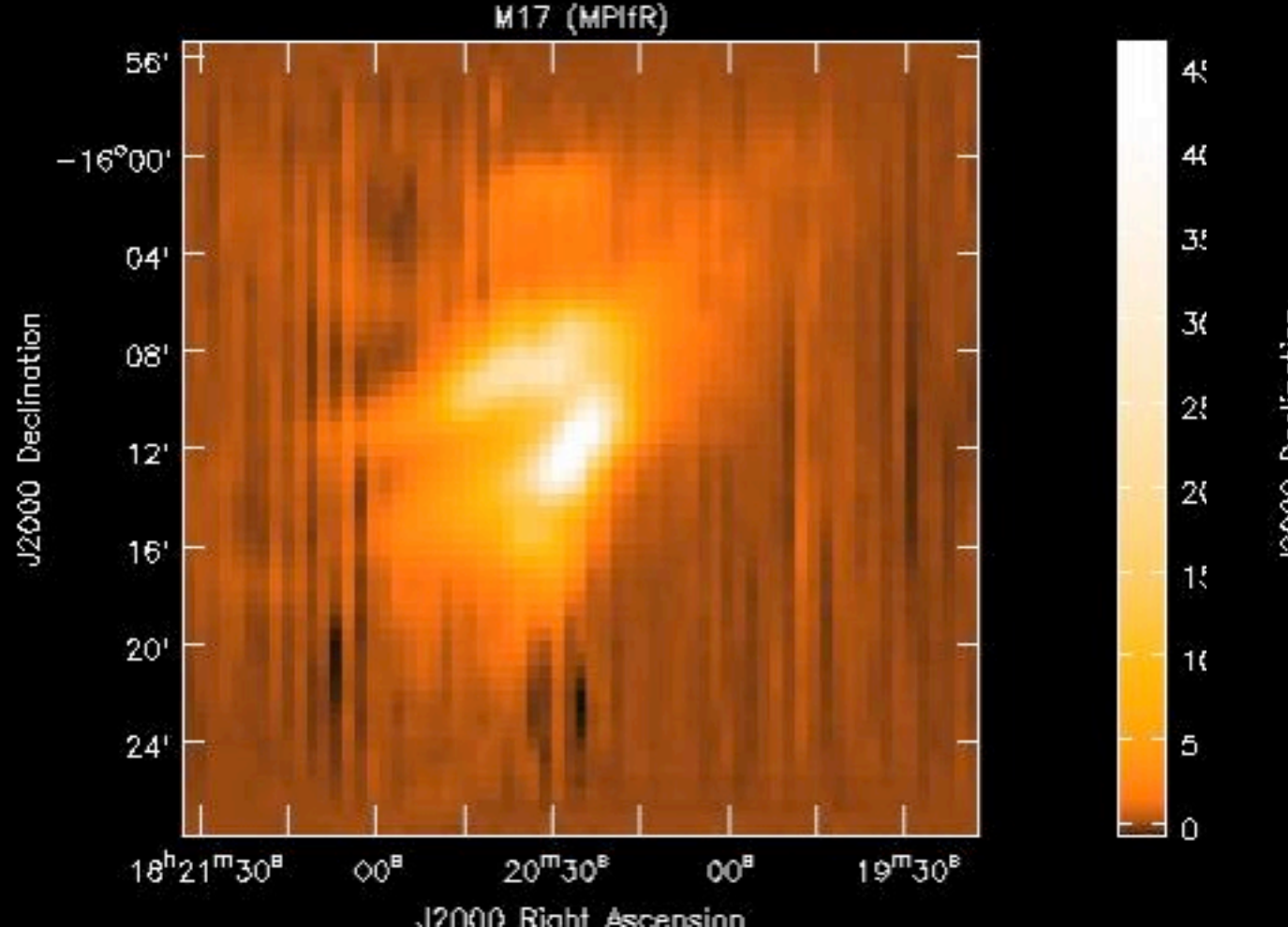
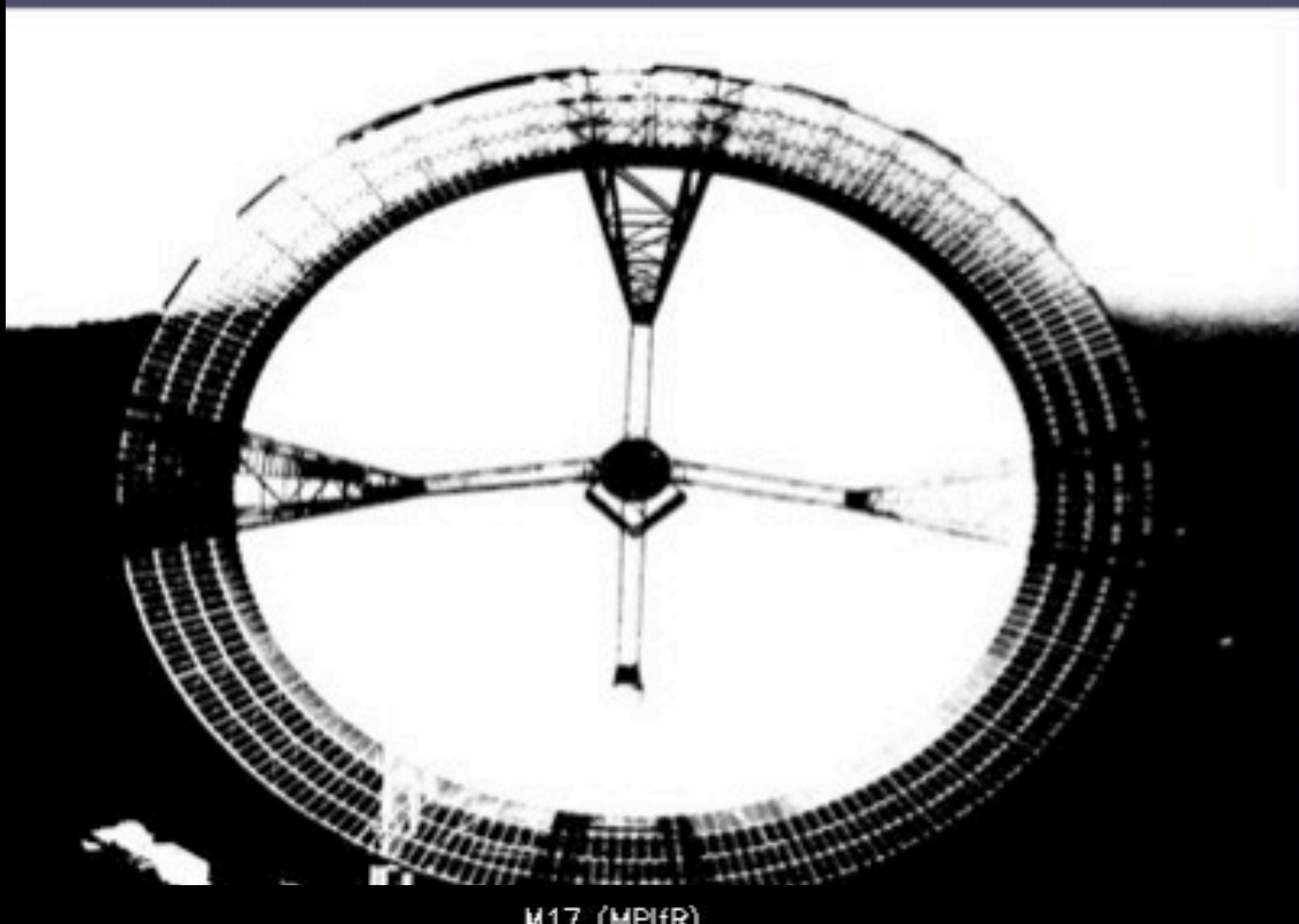
Appalachian Mountains



★ Washington D.C.

The Green Bank Telescope (GBT)





The Active Surface

RMS < 240 μ at night
the goal is 210 μ



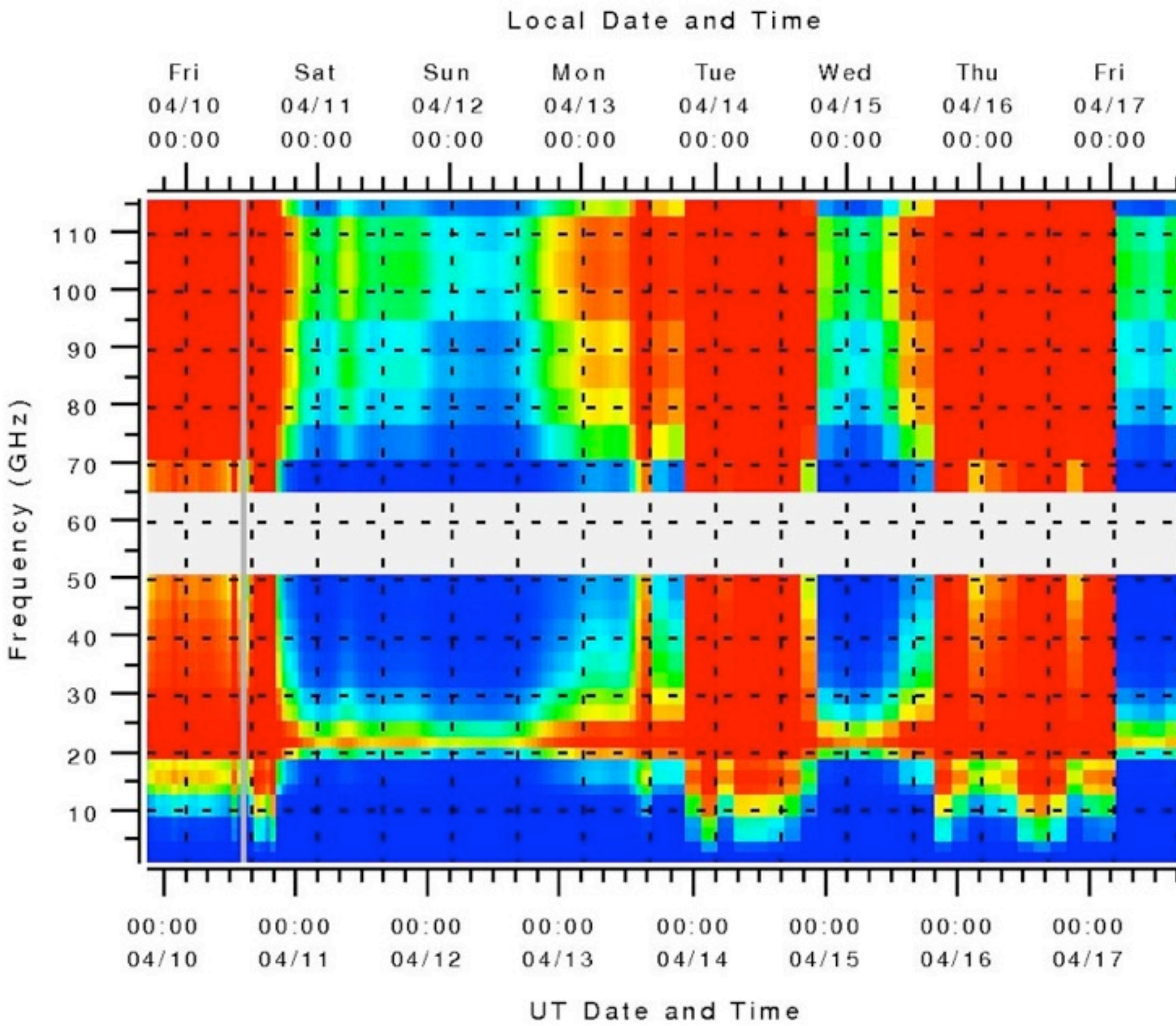
6220^h in 2014
~1/3 at $\nu \geq 18$ GHz



- Point source sensitivity of a ~120m telescope
- Point source sensitivity $\sqrt{2}$ better than VLA at $\lesssim 2$ GHz

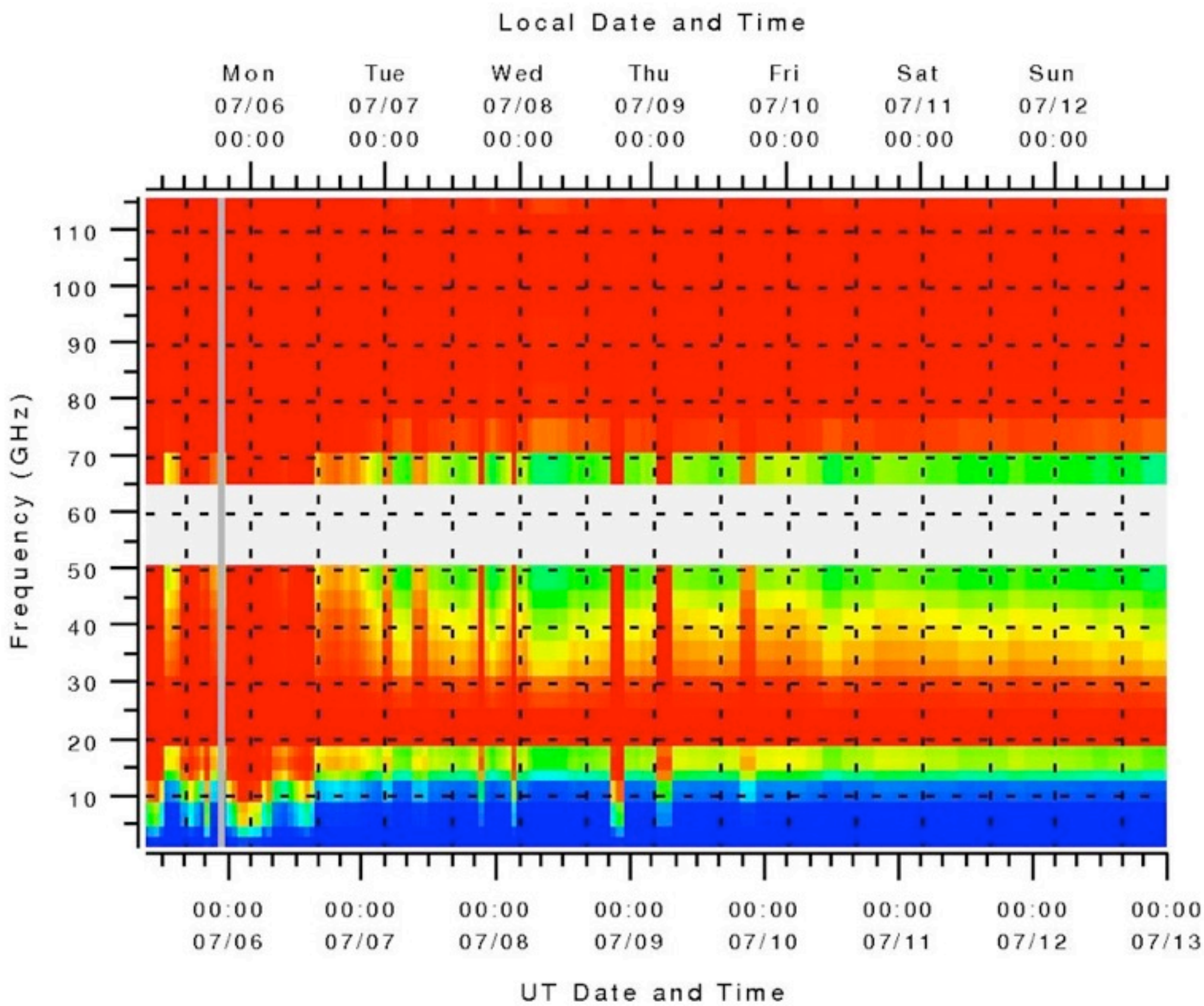
DSS Overview

Efficiencies from Atmospheric Opacities (EffAtmos)



DSS Overview

Efficiencies from Atmospheric Opacities (EffAtmos)



Research areas of most-cited GBT publications

(November 2014)

Pulsars and compact objects

Gravity and General Relativity

Galactic Hydrogen surveys

Interstellar Chemistry

The internal structure of Mercury

Evolution of spiral galaxies

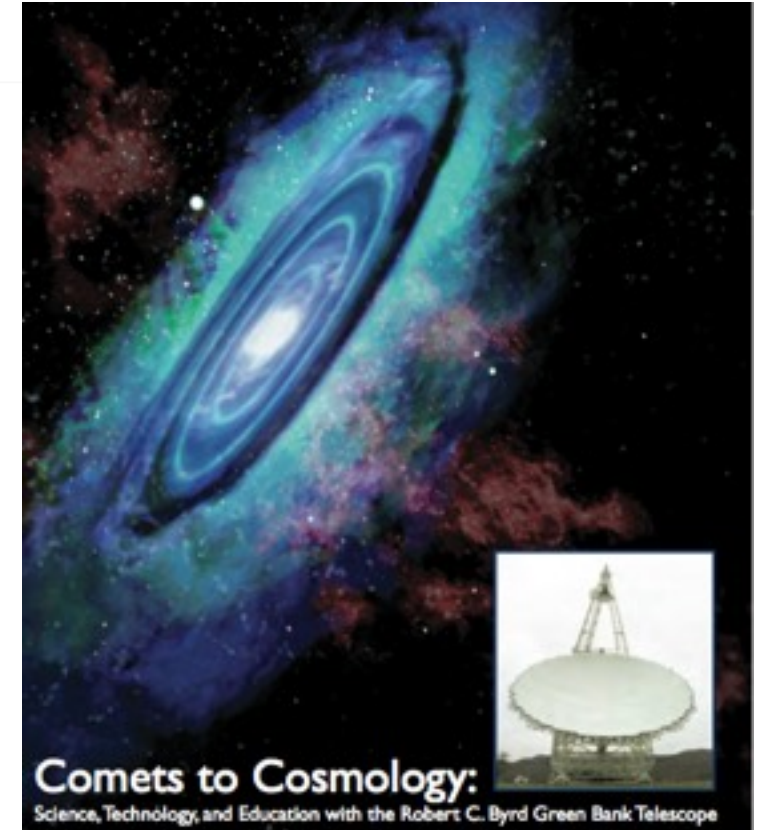
Star formation & pre-stellar objects

Studies of a binary black hole

Hydrogen content of galaxies

Molecules in highly redshifted galaxies

Anisotropies in the cosmic Infrared background



A digression on the sensitivity of radio telescopes

angular resolution $\approx \lambda/\text{Diam}$

A digression on the sensitivity of radio telescopes

angular resolution $\approx \lambda/\text{Diam}$

point source signal strength $\propto \pi r_a^2$

A digression on the sensitivity of radio telescopes

angular resolution $\approx \lambda/\text{Diam}$

point source signal strength $\propto \pi r_a^2$

time to detect $\propto (\text{signal strength})^{-2}$

A digression on the sensitivity of radio telescopes

angular resolution $\approx \lambda/\text{Diam}$

point source signal strength $\propto \pi r_a^2$

time to detect $\propto (\text{signal strength})^{-2}$

$t \propto r_a^{-4}$ (*point source*)

A digression on the sensitivity of radio telescopes

point source

$$t \propto \frac{1}{A_e^2}$$

A digression on the sensitivity of radio telescopes

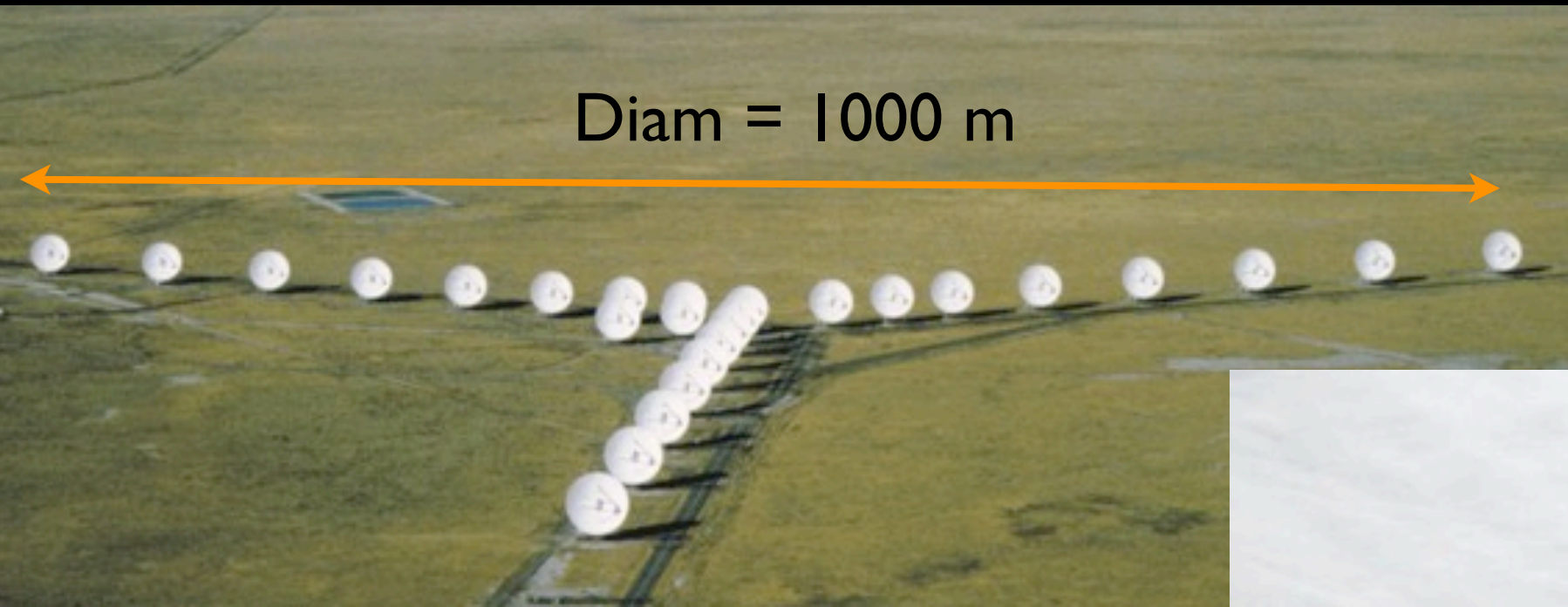
point source

$$t \propto \frac{1}{A_e^2}$$

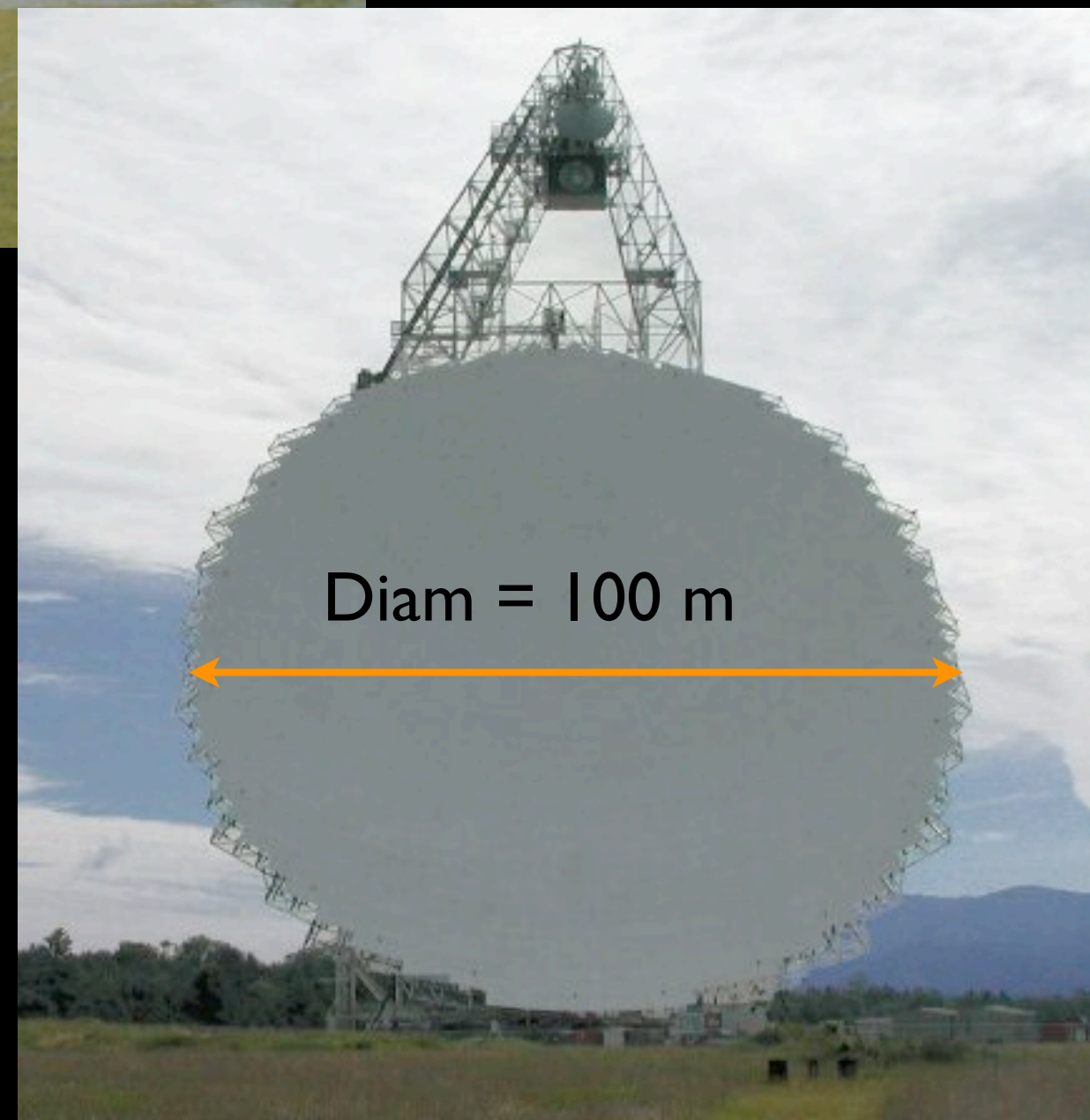
extended source

$$t \propto f^2 \propto \frac{\text{Diam}^4}{A_e^2}$$

A digression on the sensitivity of radio telescopes



$$t \propto f^2 \propto \frac{Diam^4}{A_e^2}$$



A digression on the sensitivity of radio telescopes

Instrument	f^2	21cm HPBW
GBT	I	9.1'
Arecibo	I	3.2'
VLA-D	$\sim 10^4$	46"
VLA-C	$\sim 10^6$	14"
VLA-B	$\sim 10^8$	4.3"
ASKAP	$\sim 10^6$	

$$t \propto f^2 \propto \frac{Diam^4}{A_e^2}$$

A digression on the sensitivity of radio telescopes

Instrument	f^2	21cm HPBW
GBT	I	9.1'
Arecibo	I	3.2'
VLA-D	$\sim 10^4$	46"
VLA-C	$\sim 10^6$	14"
VLA-B	$\sim 10^8$	4.3"
....	...	

For a given collecting area, the brightness sensitivity is always greatest for a filled aperture

$$t \propto f^2 \propto \frac{\text{Diam}^2}{A_e^2}$$

A digression on the sensitivity of radio telescopes

Instrument	f^2	21cm HPBW
GBT	I	9.1'
Arecibo	I	3.2'
VLA-D	$\sim 10^4$	46"
VLA-C	$\sim 10^6$	14"
VLA-B	$\sim 10^8$	4.3"
....	...	

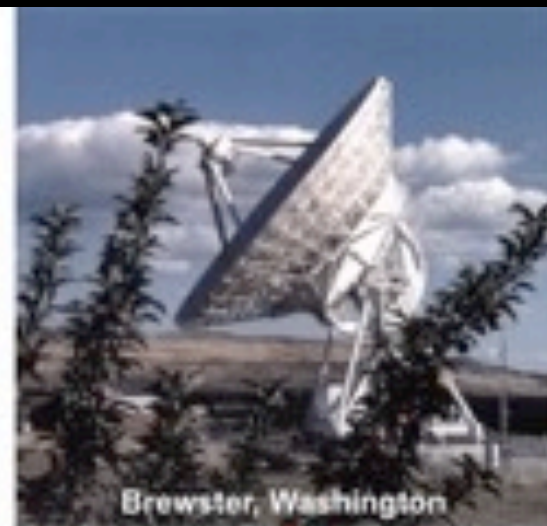
For a given collecting area, the brightness sensitivity is always greatest for a filled aperture

This is not related to the issue of missing short spacings

VLBA Limited to $T > 10^5$ K



Owens Valley, California



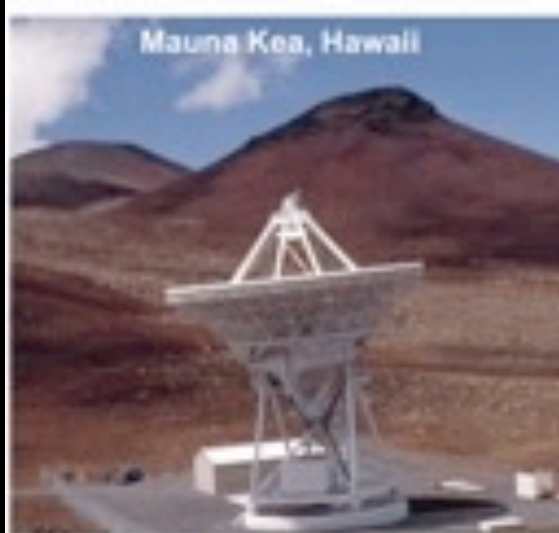
Brewster, Washington



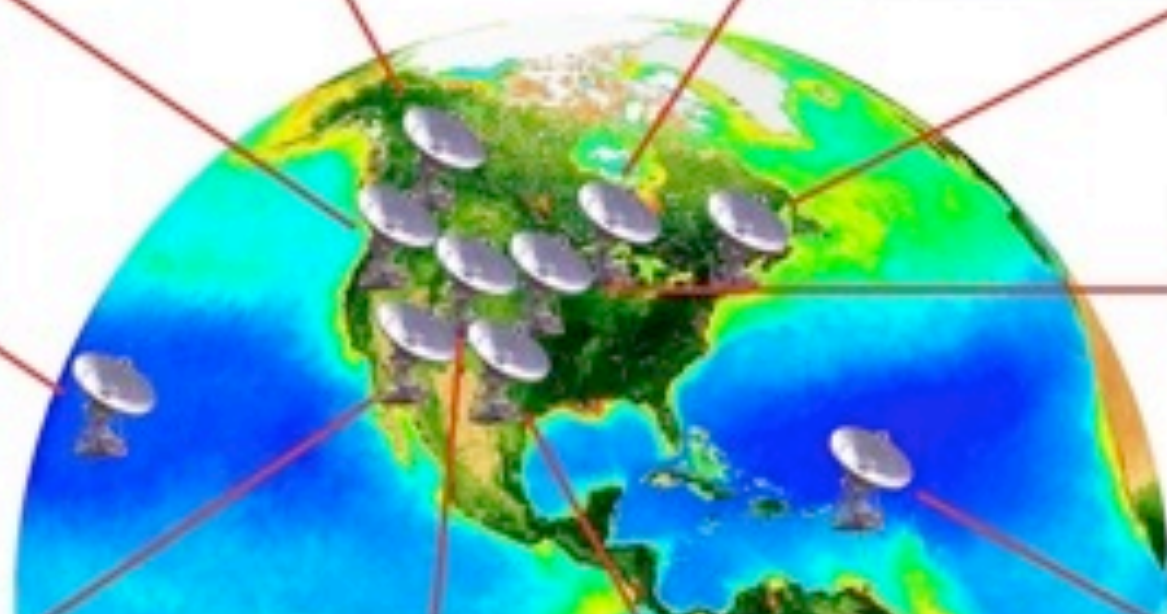
North Liberty, Iowa



Hancock, New Hampshire



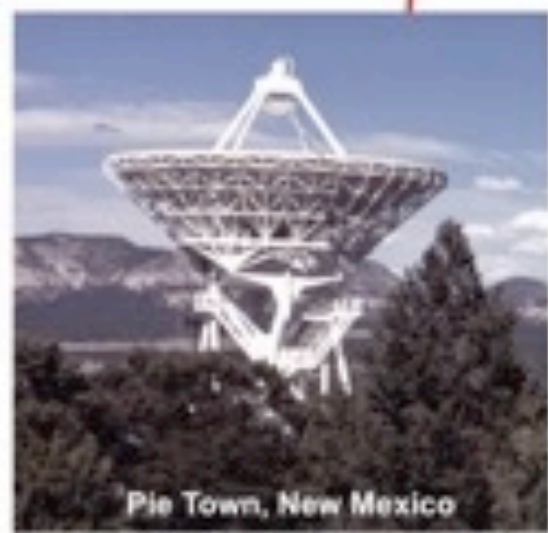
Mauna Kea, Hawaii



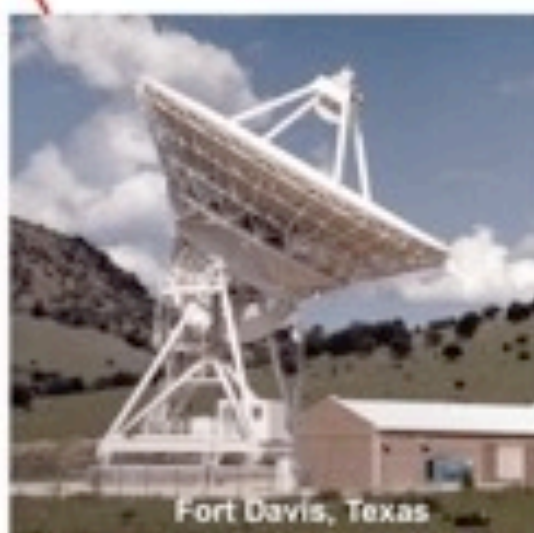
Los Alamos, New Mexico



Kitt Peak, Arizona



Pie Town, New Mexico



Fort Davis, Texas



St. Croix, Virgin Islands

Bi-static radar studies with Arecibo

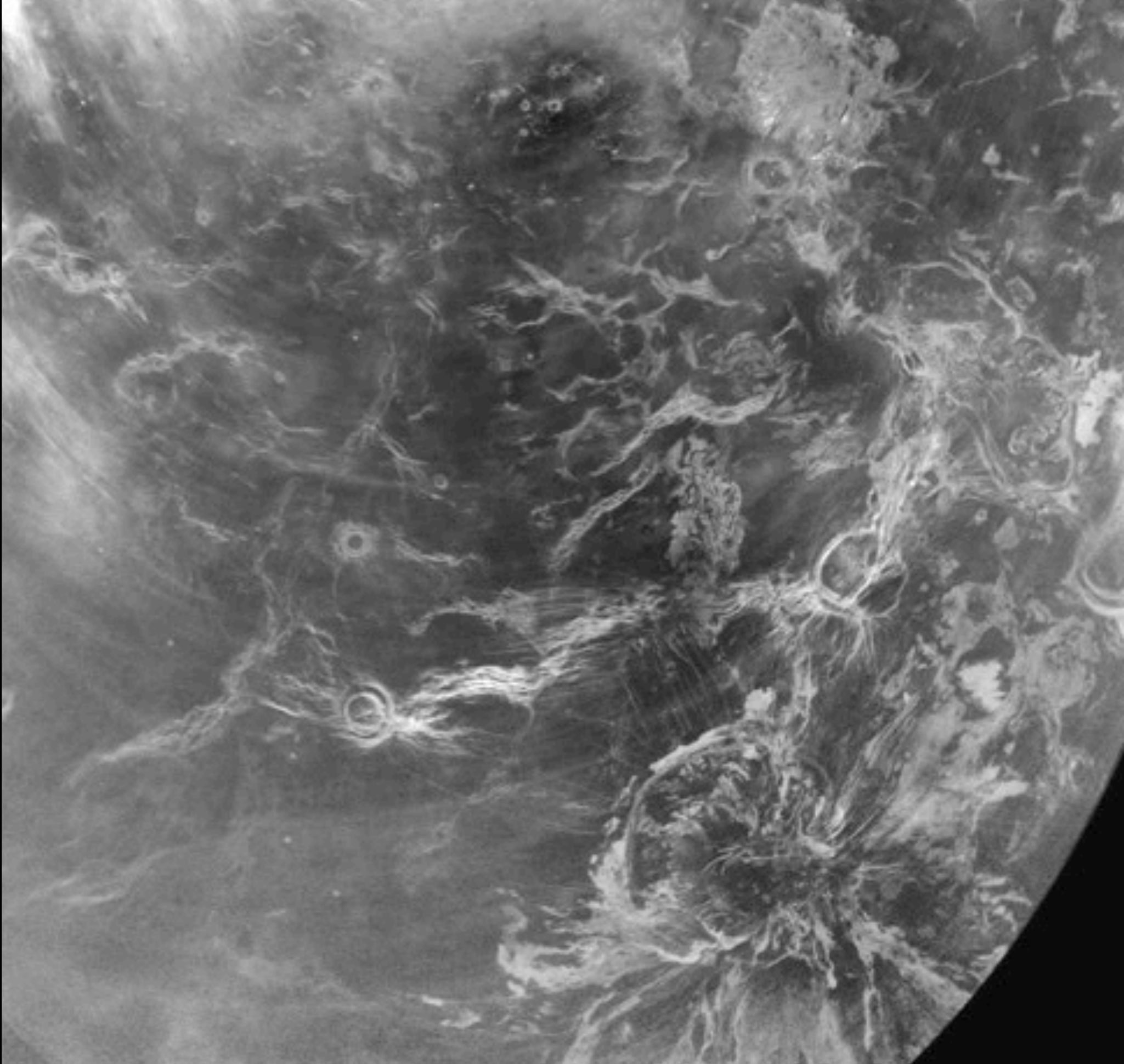


GBT receiving

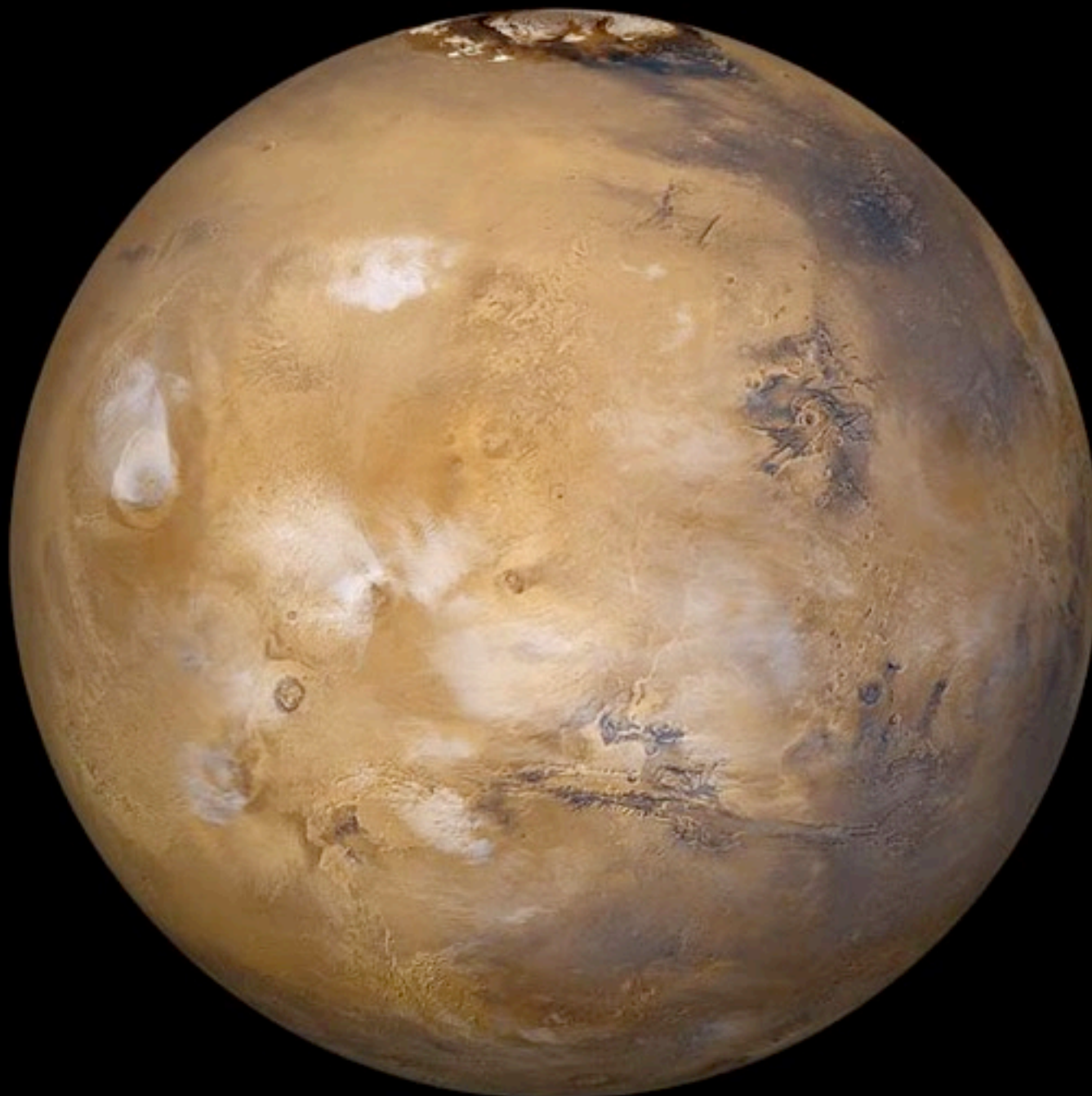


VENUS RADAR

B. Campbell



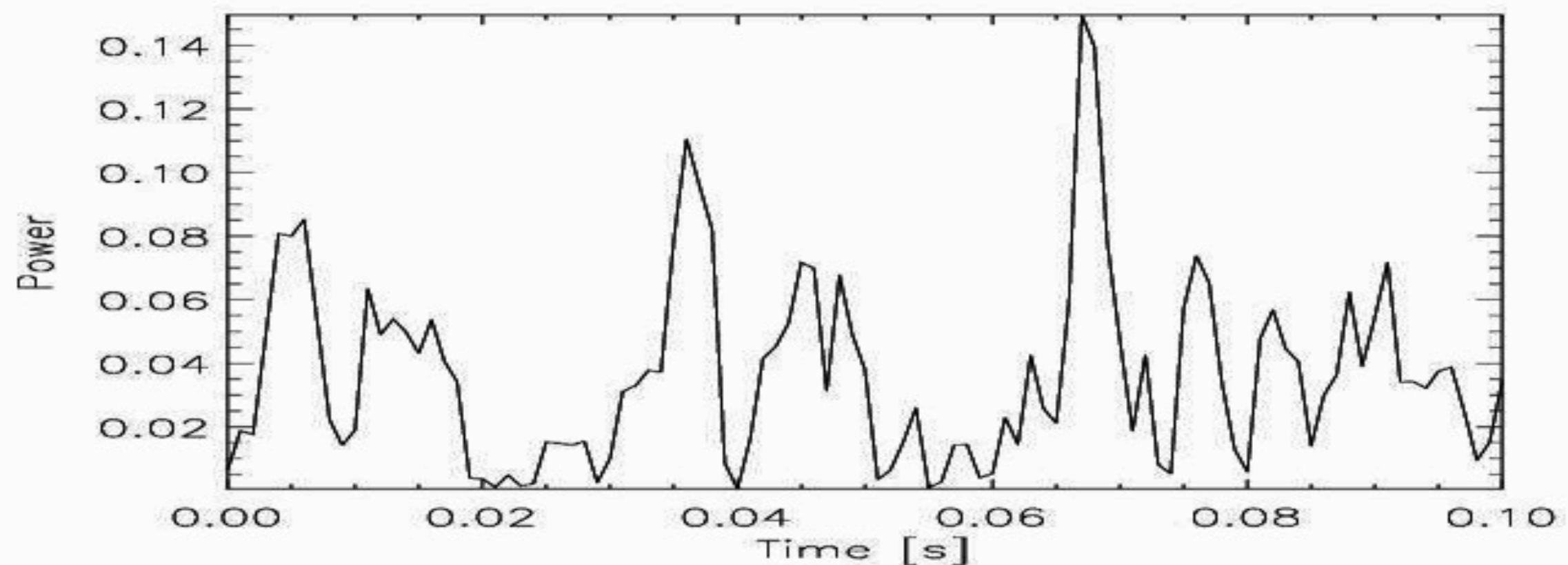
A radar return is speckled



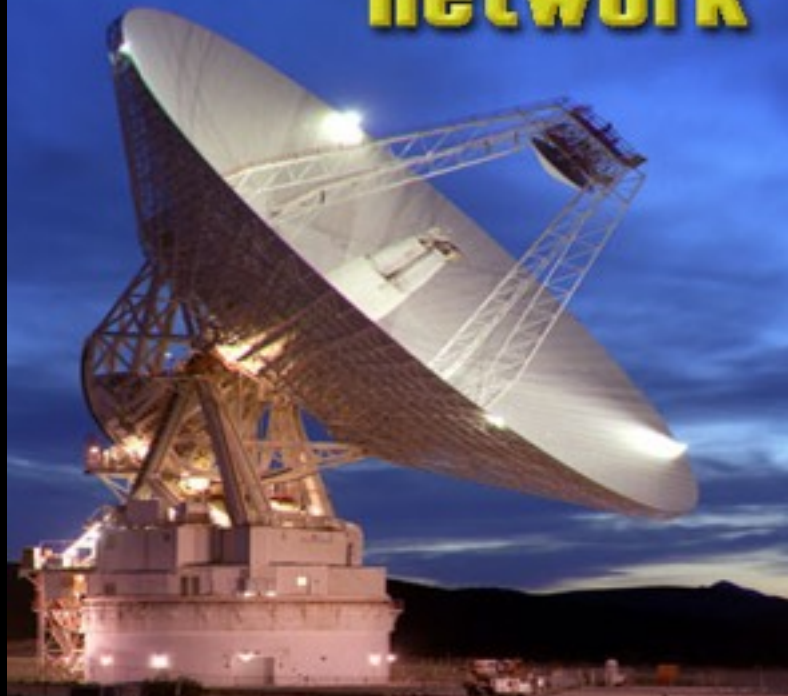
A radar return is speckled



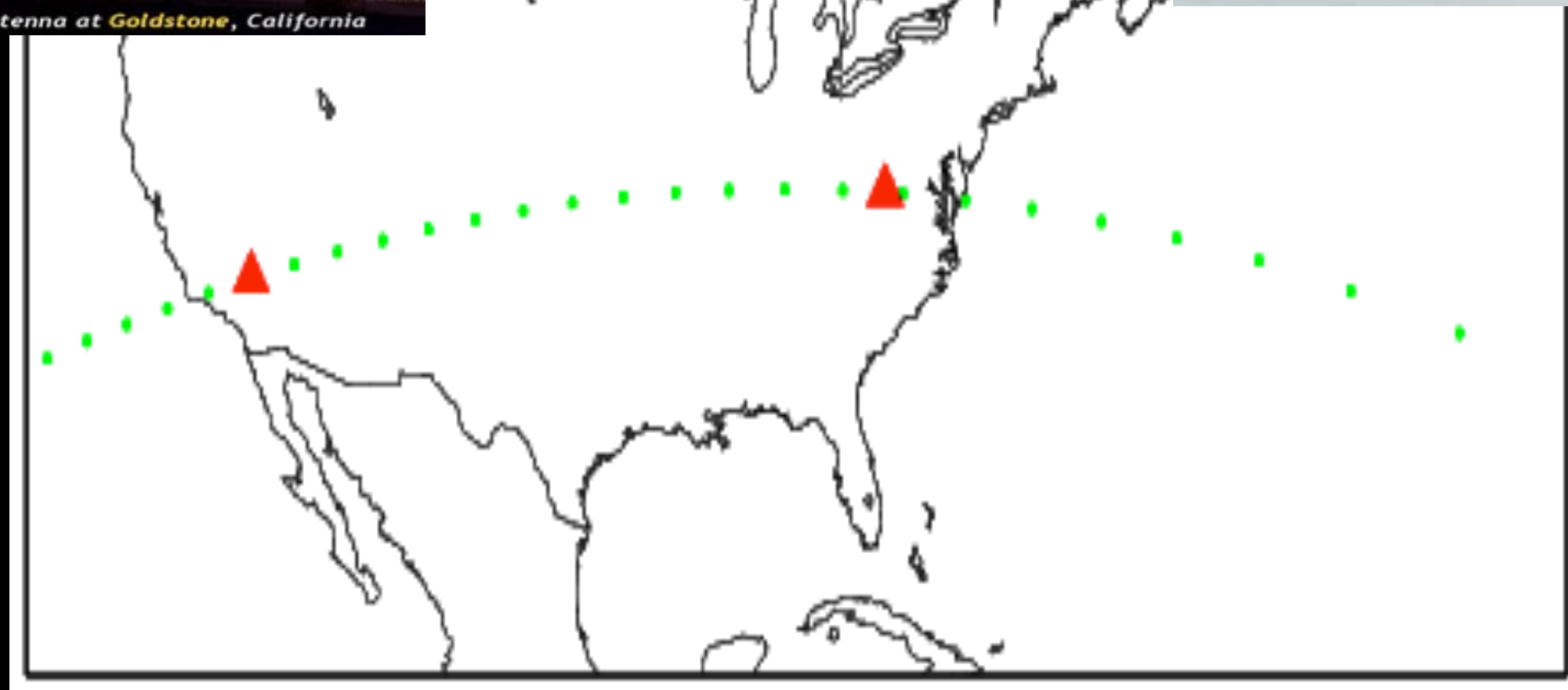
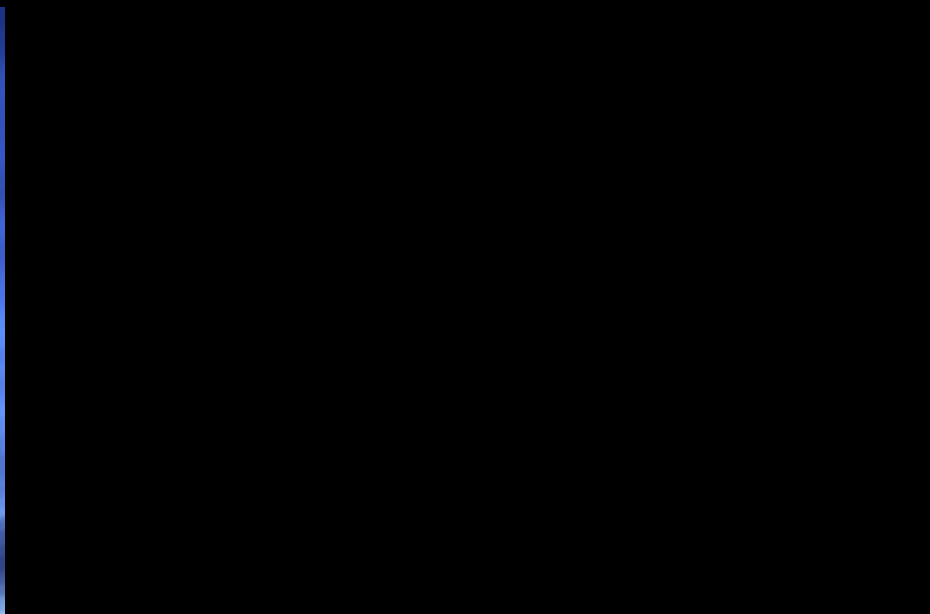
The radar return is speckled



deep space network

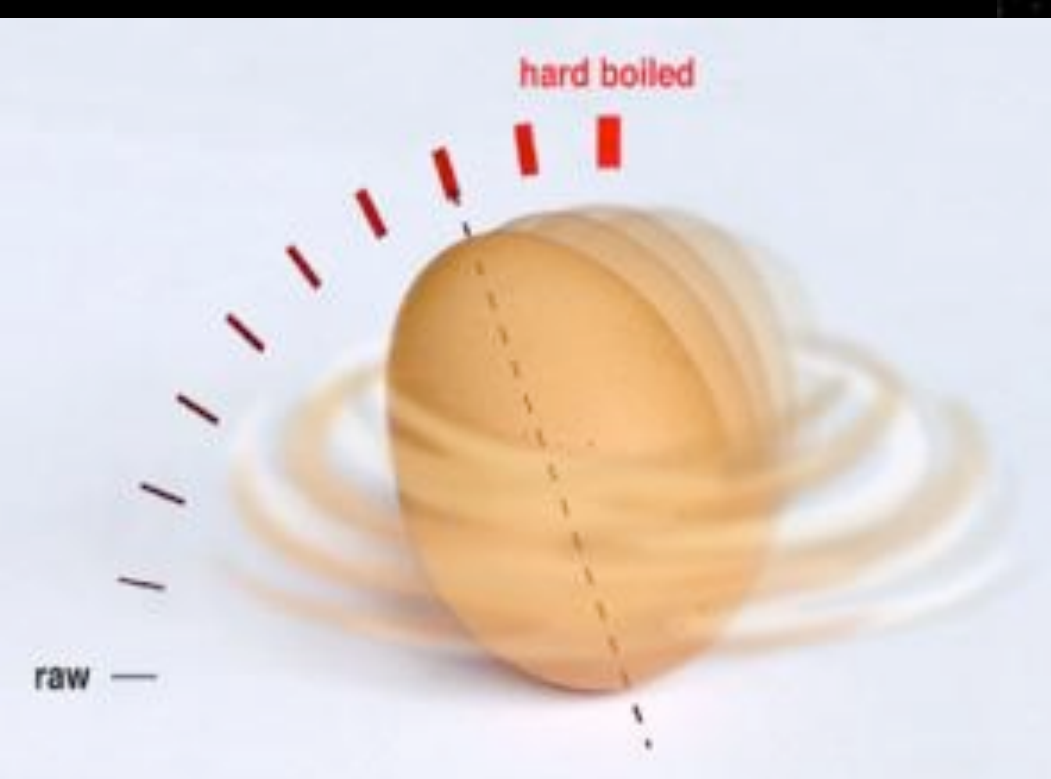
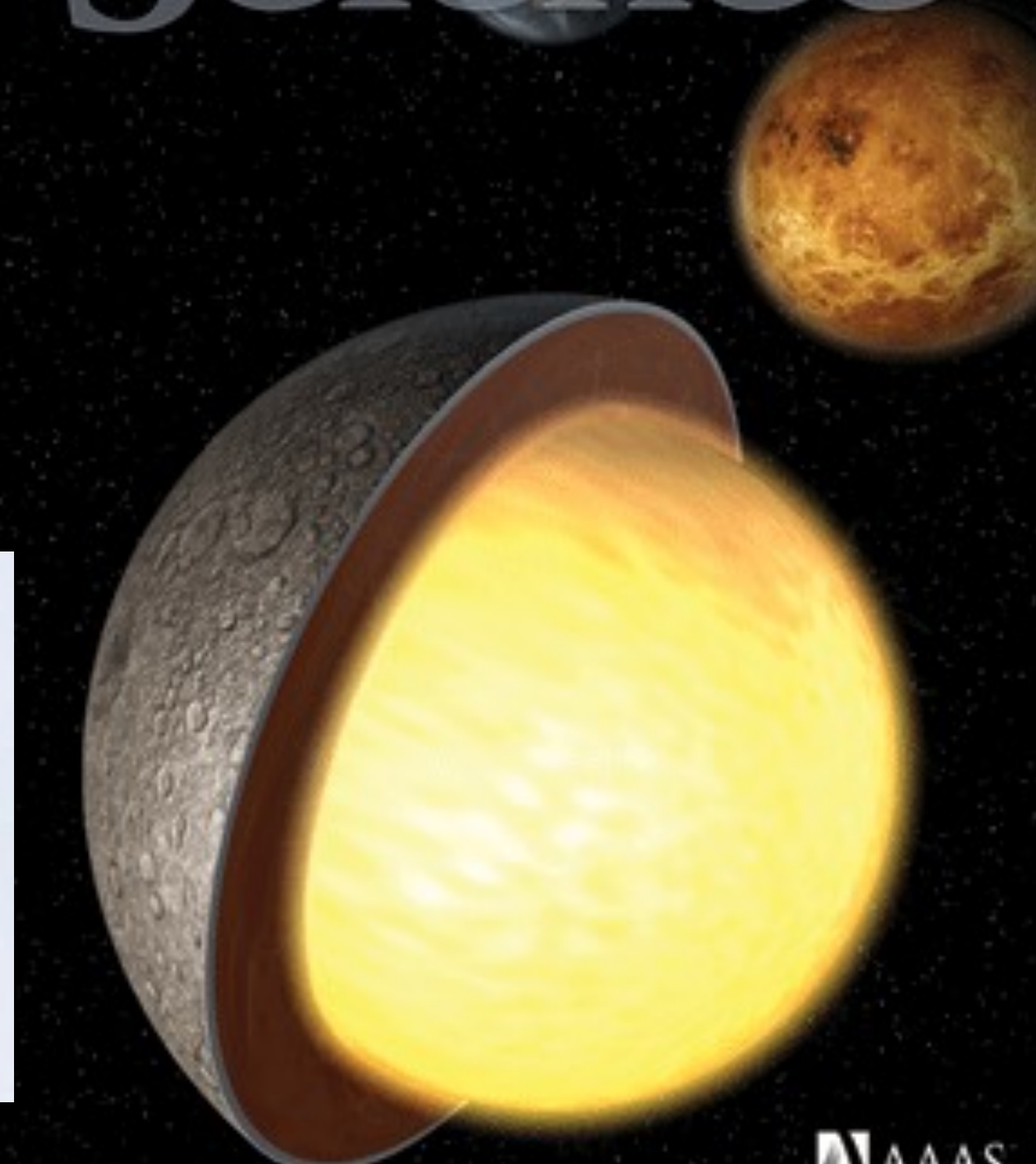


70-meter antenna at *Goldstone, California*



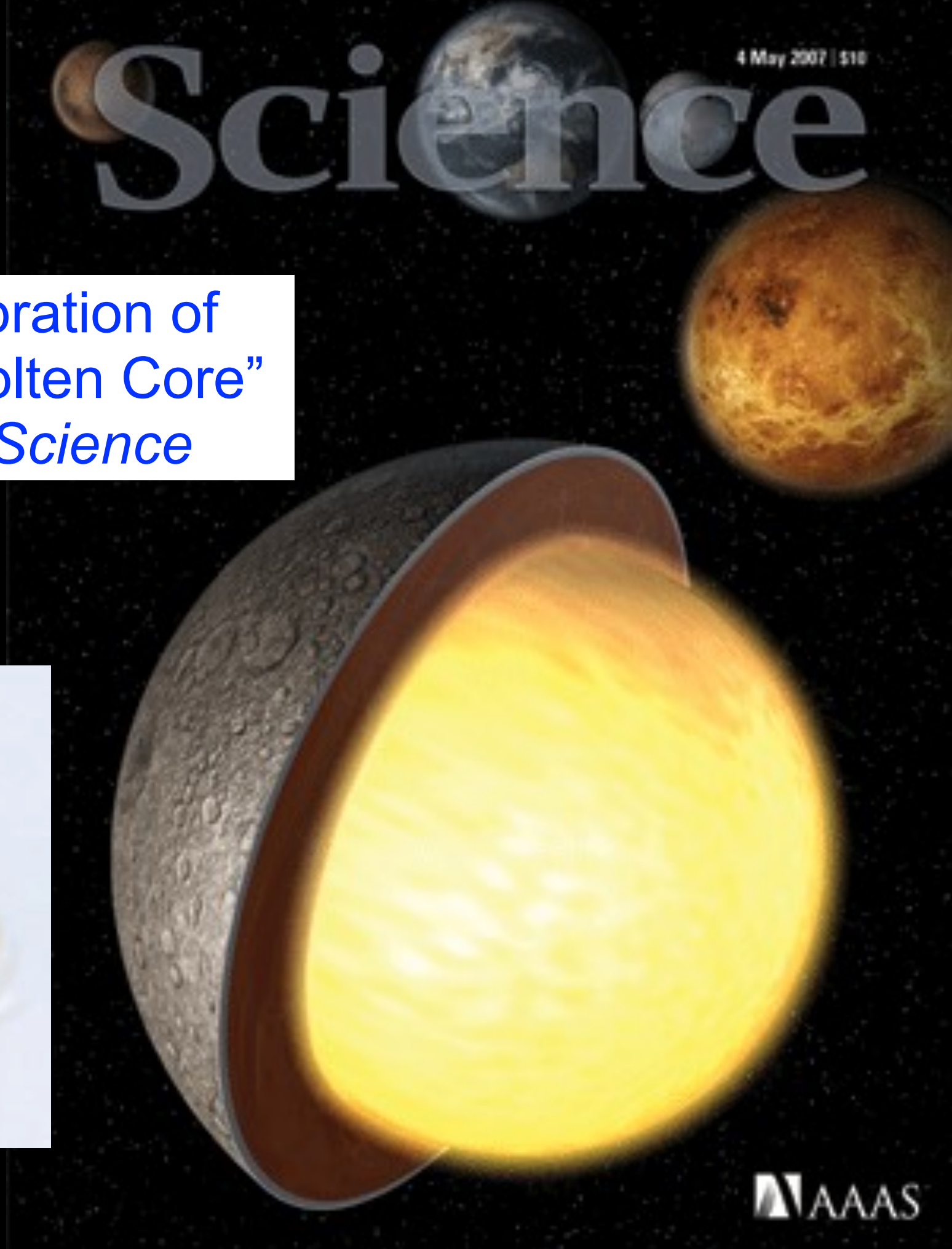
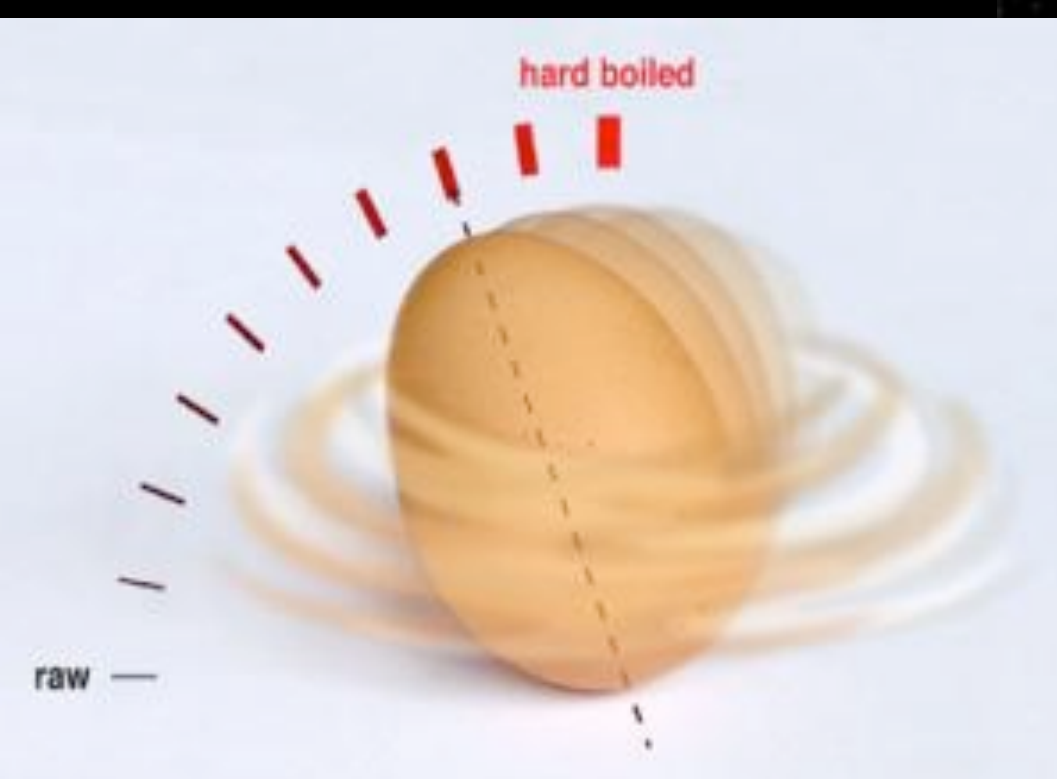
4 May 2007 | \$10

Science

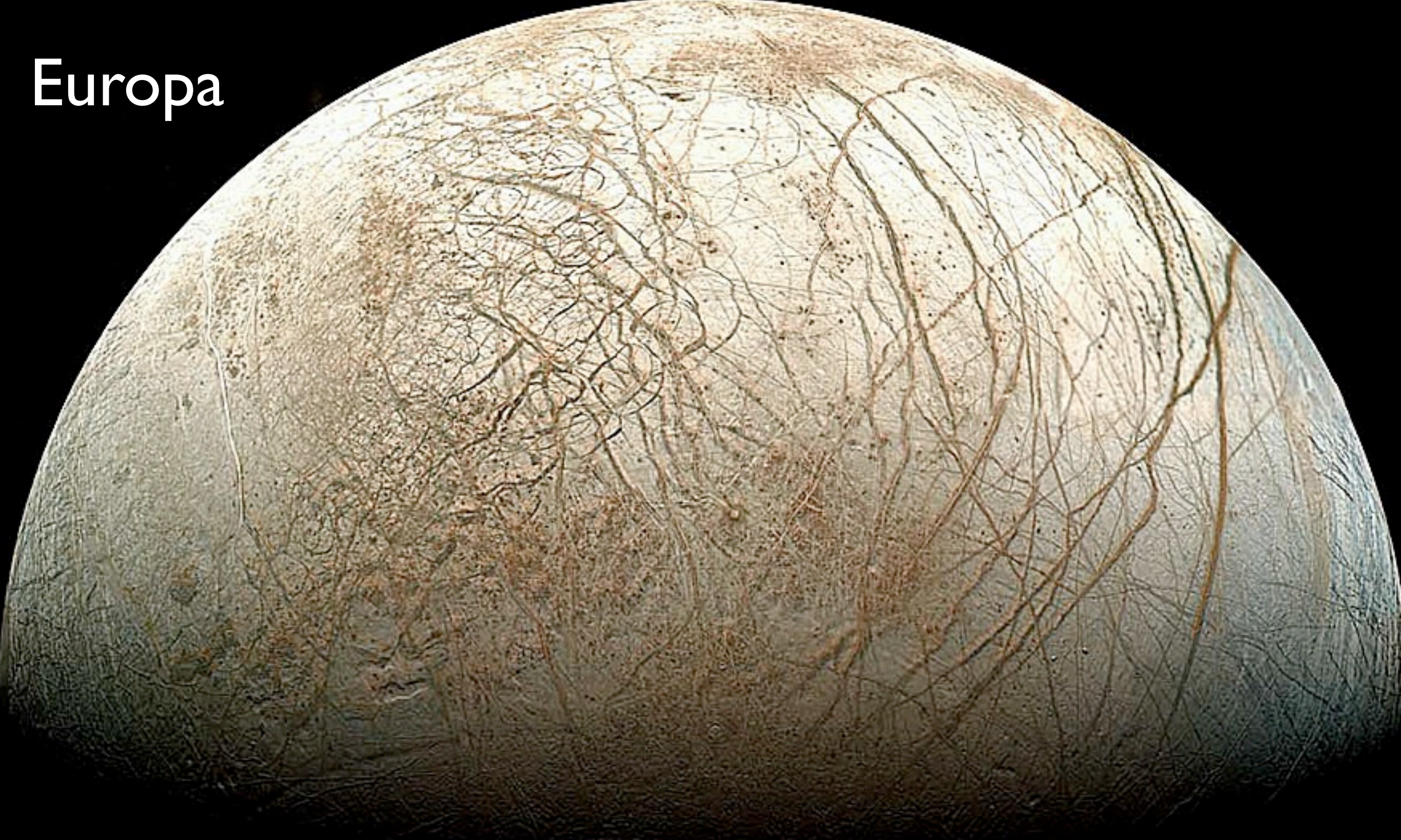


AAAS

“Large Longitude Libration of
Mercury Reveals a Molten Core”
Margot et al. 2007 Science

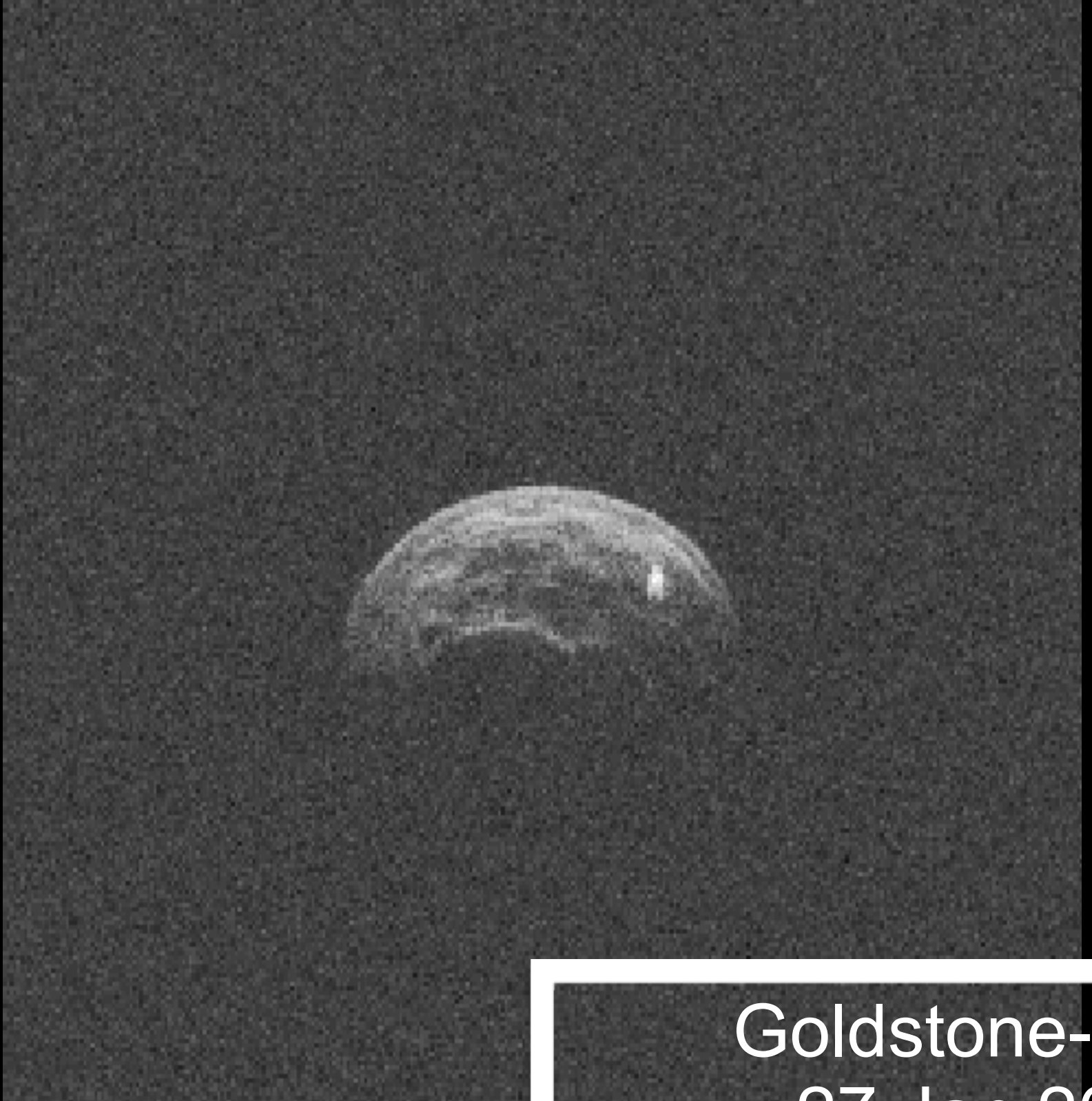


Europa



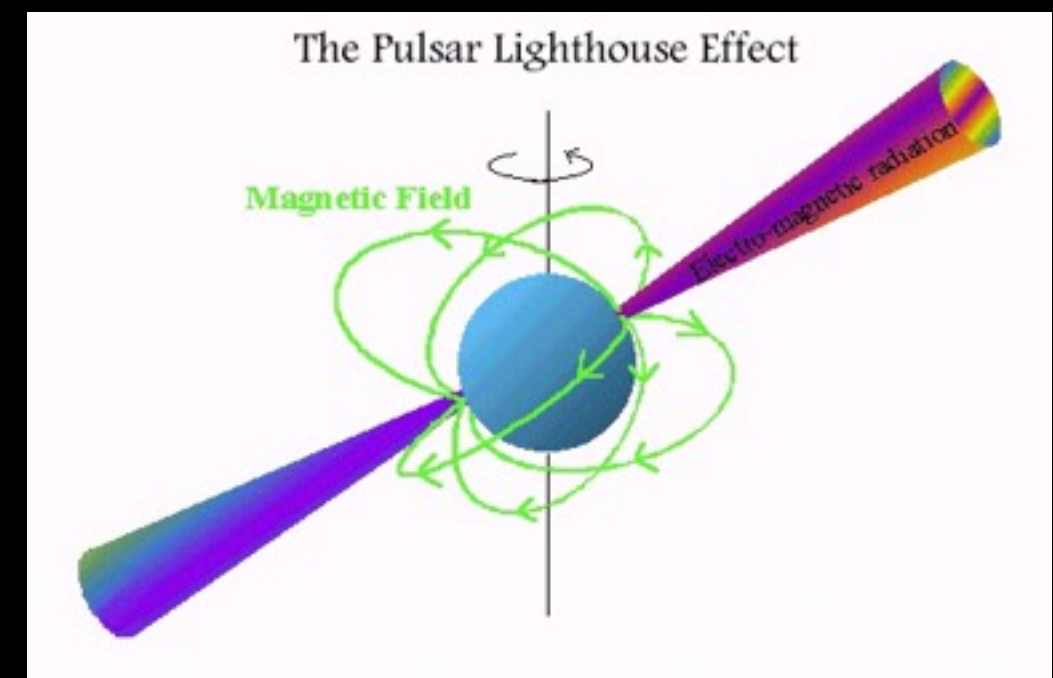
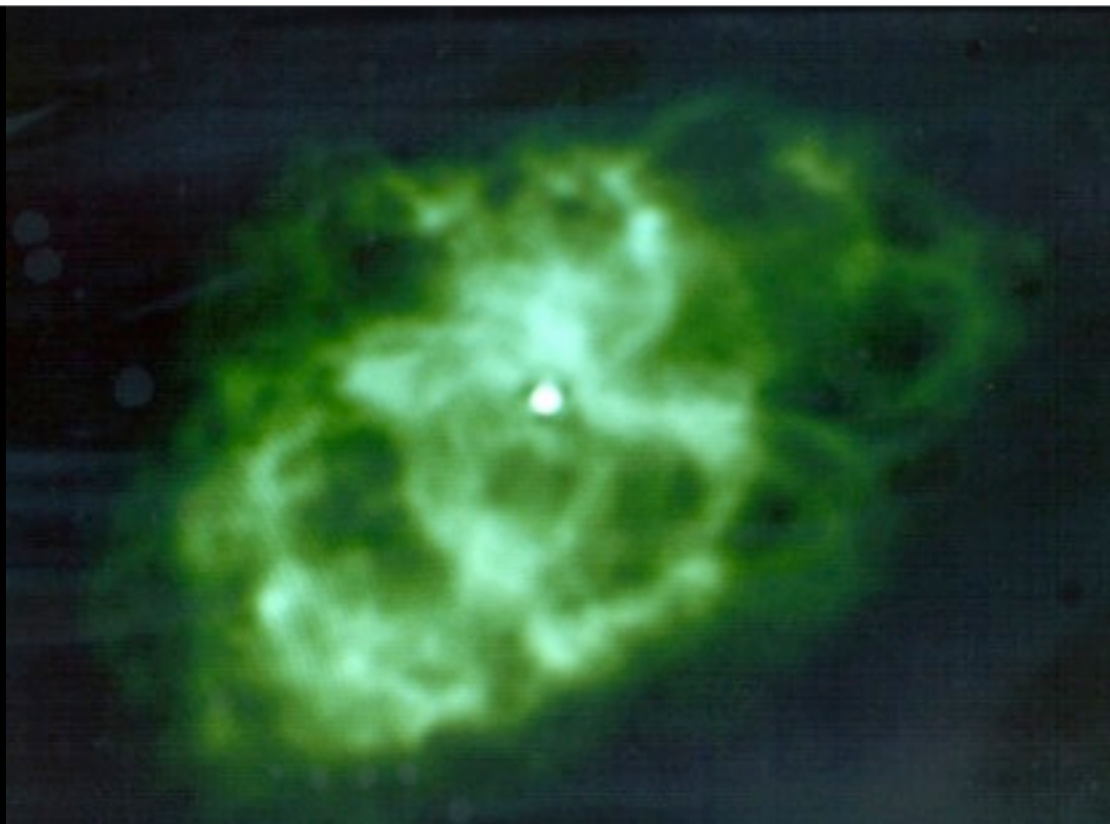
Chelyabinsk, Russia -- Feb. 15, 2013



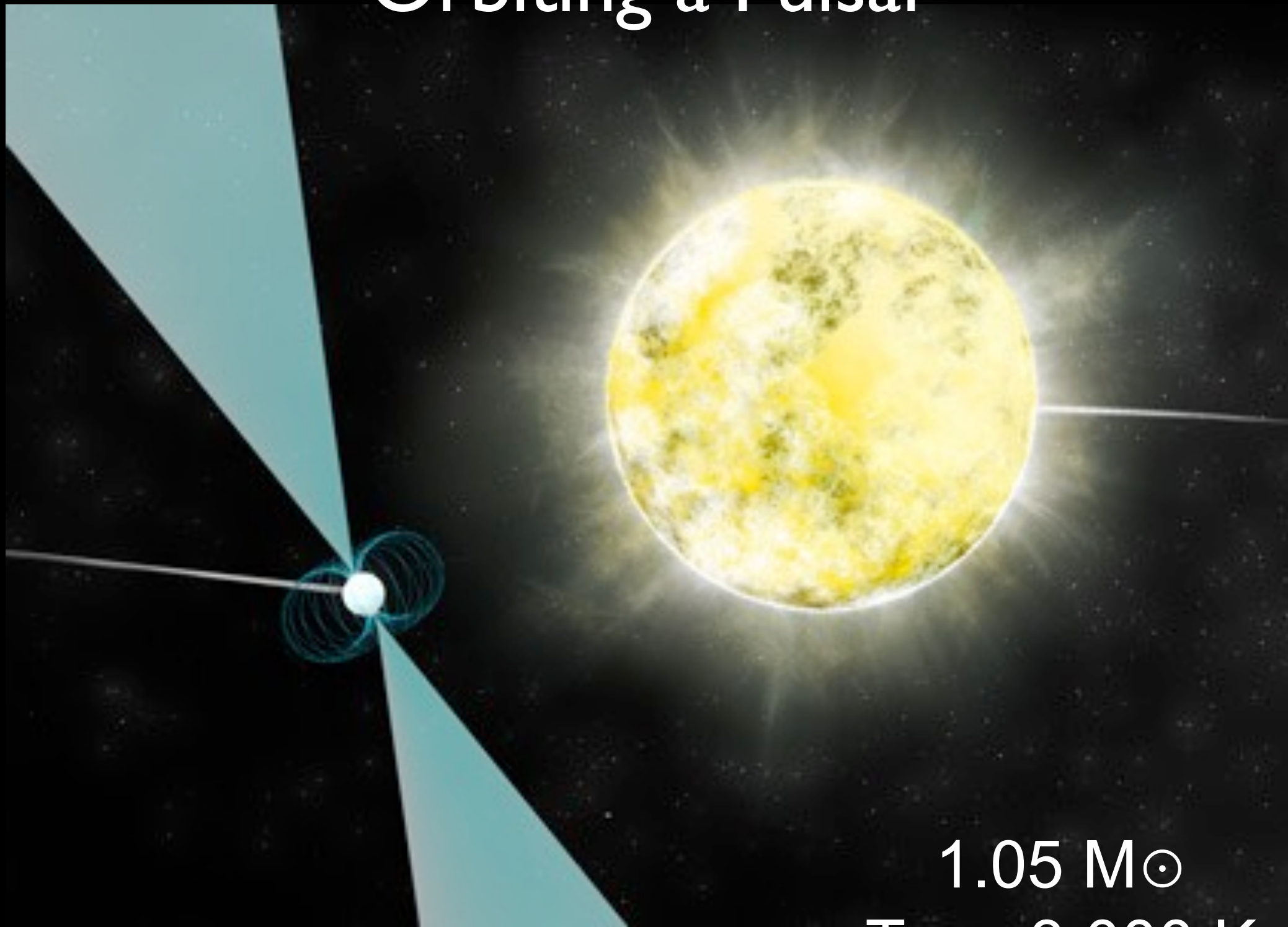


Goldstone-GBT
27 Jan 2015
Asteroid 2004BL86

The Pulsar Renaissance
Fastest Pulsar
Most Massive Pulsar
Pulsars in Globular Clusters
Tests of General Relativity
Relativistic Spin Precession
Pulsar in a three-body system
Coolest white dwarf star (a diamond as big as the Ritz)



A Solid Carbon “Diamond” Star Orbiting a Pulsar

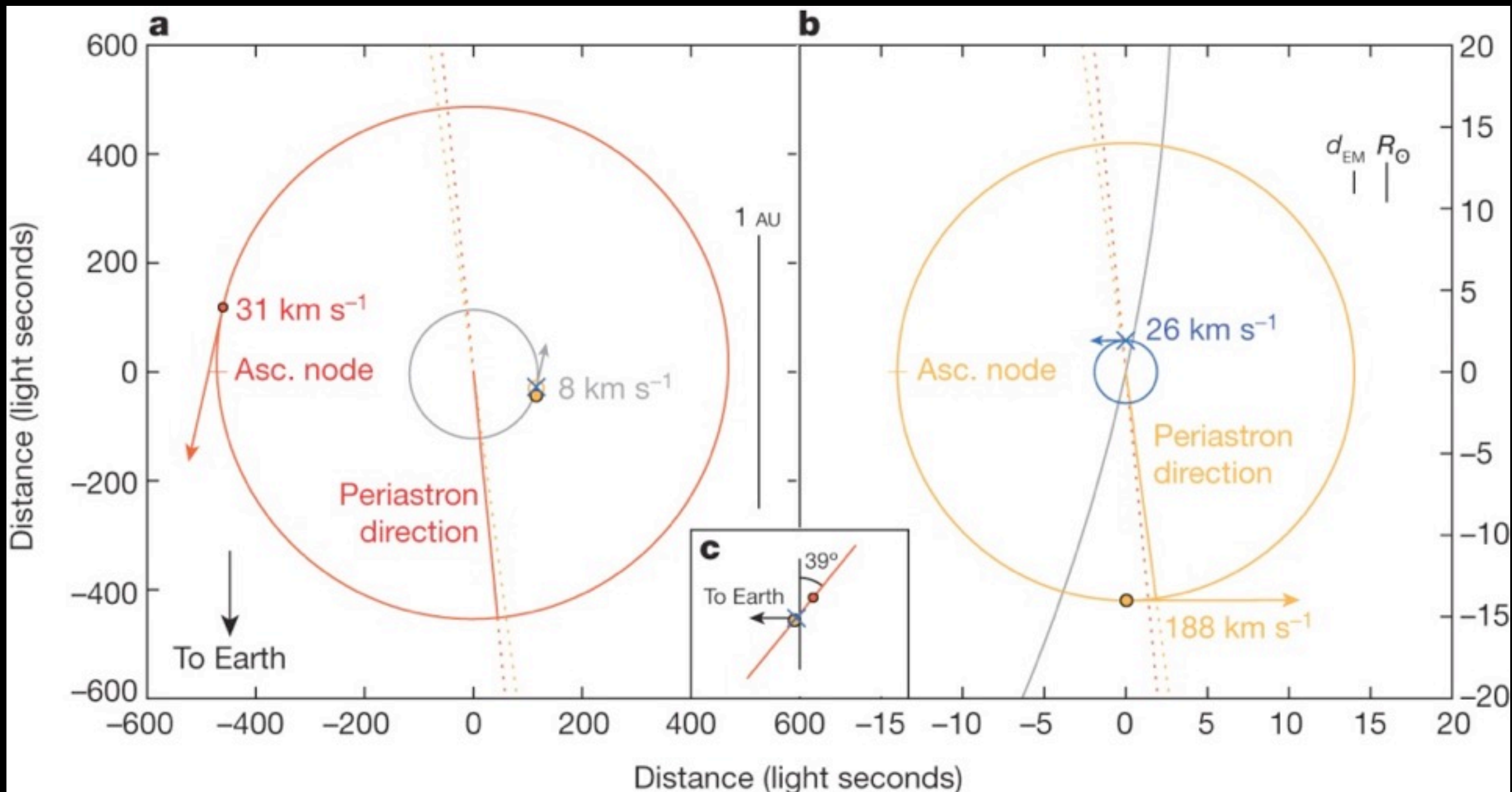


$1.05 M_{\odot}$
 $T_{\text{eff}} < 3\,000 \text{ K}$

A Pulsar in a Triple System

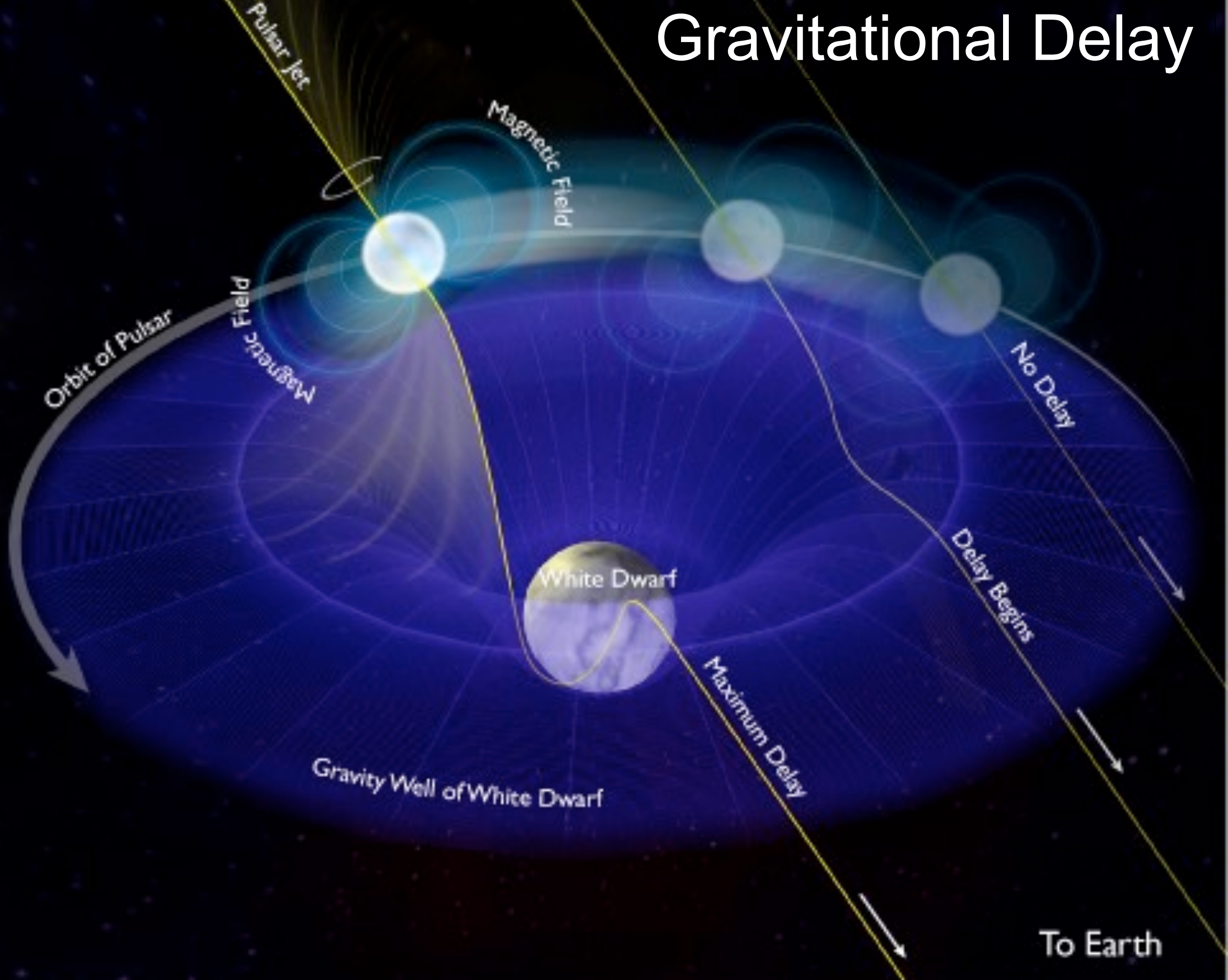
ARECIBO+ GBT

Ransom et al. Nature (2014)

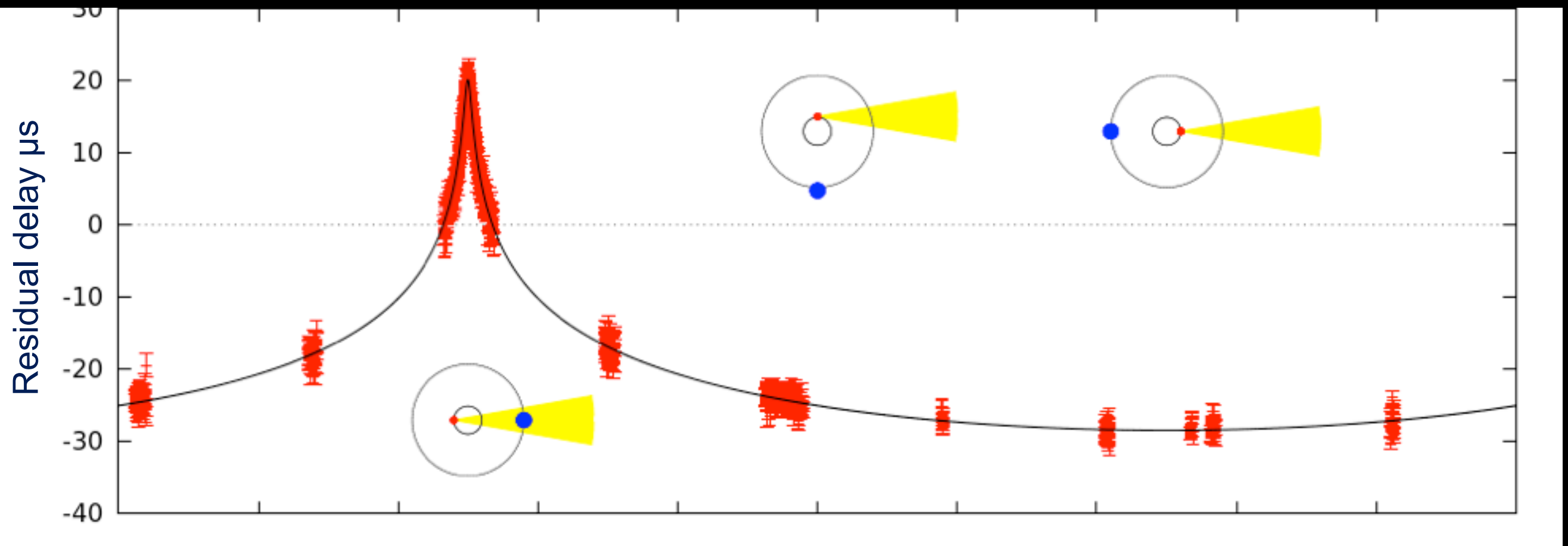


Testing the Equivalence Principle

Gravitational Delay



GBT measurements of the radio pulsar J1614-2230



Demorest et al. (2010)

TESTING THEORIES OF GRAVITATION USING 21-YEAR TIMING OF PULSAR BINARY J1713+0747

ZHU^{1,14}, I. H. STAIRS¹, P. B. DEMOREST¹⁷, D. J. NICE³, J. A. ELLIS^{4,5}, S. M. RANSOM², Z. ARZOUMANIAN^{6,7}, K. CROWDOLCH⁸, R. D. FERDMAN⁹, E. FONSECA¹, M. E. GONZALEZ^{1,10}, G. JONES¹¹, M. JONES¹², M. T. LAM⁸, L. LEVIN^{12,16}, M. McLAUGHLIN¹², T. PENNUCCI¹⁵, K. STOVALL¹³, J. SWIGGUM¹²

Draft version April 3, 2015

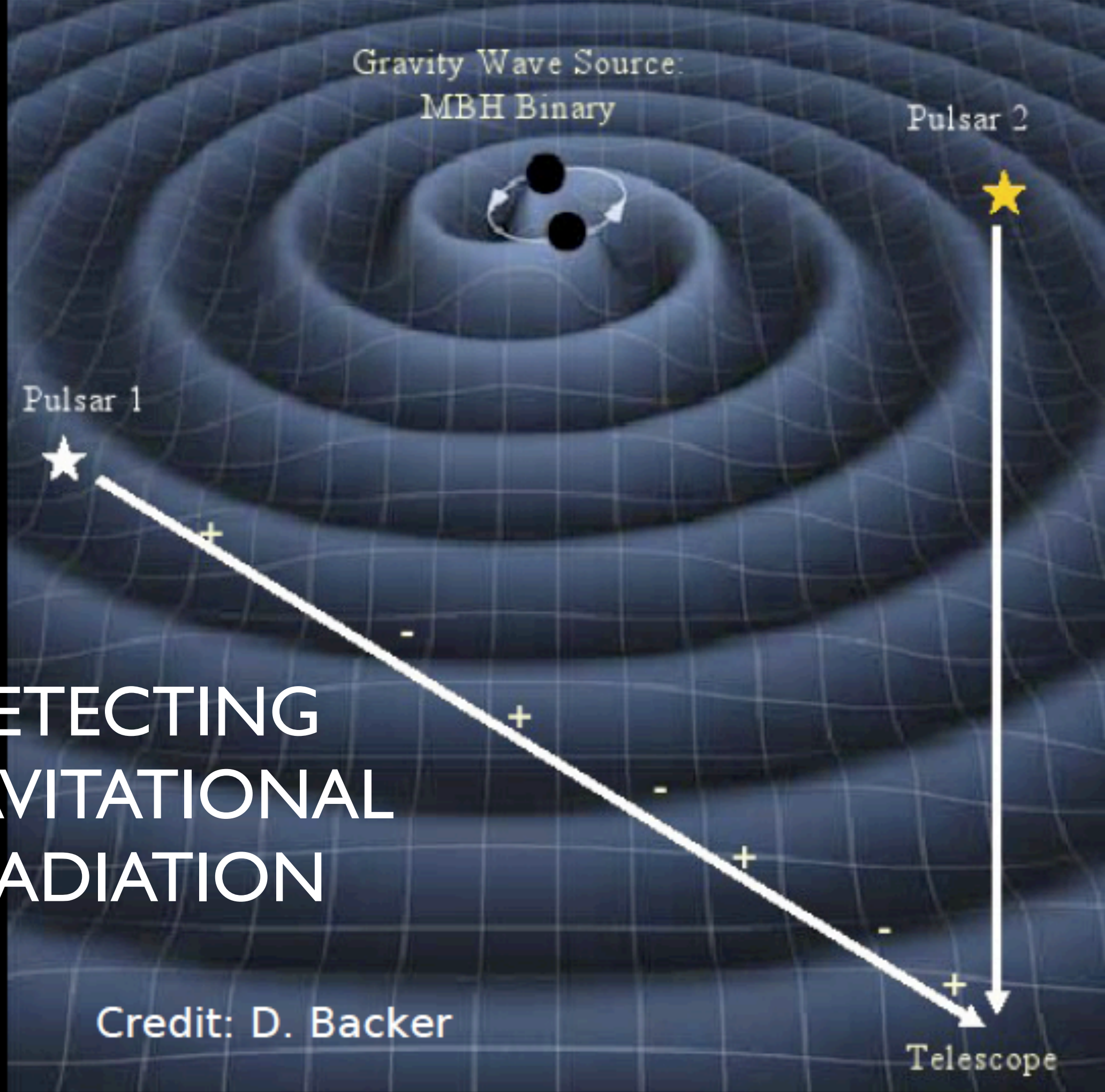
ABSTRACT

We report 21-yr timing of one of the most precise pulsars: PSR J1713+0747. The pulsar's pulse times of arrival are well modeled, with residuals having weighted root mean square of ~ 92 ns, by a comprehensive pulsar binary model including the mass and three-dimensional orbit of its white dwarf companion and a noise model that incorporates short- and long-timescale correlated noise such as jitter and red noise. The new dataset allows us to update and greatly improve previous measurements of the system properties, including the masses of the neutron star ($1.31 \pm 0.11 M_{\odot}$) and white dwarf ($0.286 \pm 0.012 M_{\odot}$) as well as their parallax distance 1.15 ± 0.03 kpc. We measured a change in the observed orbital period of PSR J1713+0747, which we attribute to the relative motion of the binary system and the Earth. The intrinsic change in orbital period, P_b^{Int} , is -0.20 ± 0.17 ps s⁻¹, not distinguishable from zero. This result, combined with the measured P_b^{Int} of other pulsars, can place limits on potential changes in the gravitational constant G as predicted in some alternative theories of gravitation. We found that \dot{G}/G is consistent with zero [$(-0.6 \pm 1.1) \times 10^{-12}$ yr⁻¹, 95% confidence level] and changes at least a factor of 31 (99.7% confidence level) more slowly than the average expansion rate of the Universe. This is the best \dot{G}/G limit from pulsar binary systems. The P_b^{Int} of pulsar binaries can also place limits on the putative coupling constant for dipole gravitational radiation κ_D . We found at 95% confidence level $\kappa_D = (-0.9 \pm 3.3) \times 10^{-4}$, consistent with zero. Finally, the nearly circular orbit of this pulsar binary allows us to constrain statistically strong-field post-Newtonian parameters Δ , which describes the violation of strong equivalence principle, and $\hat{\alpha}_3$, which describes a breaking of both Lorentz invariance in gravitation and conservation of momentum. We found at 95% confidence level $\Delta < 0.01$ and $\hat{\alpha}_3 < 2 \times 10^{-20}$ based on PSR J1713+0747.

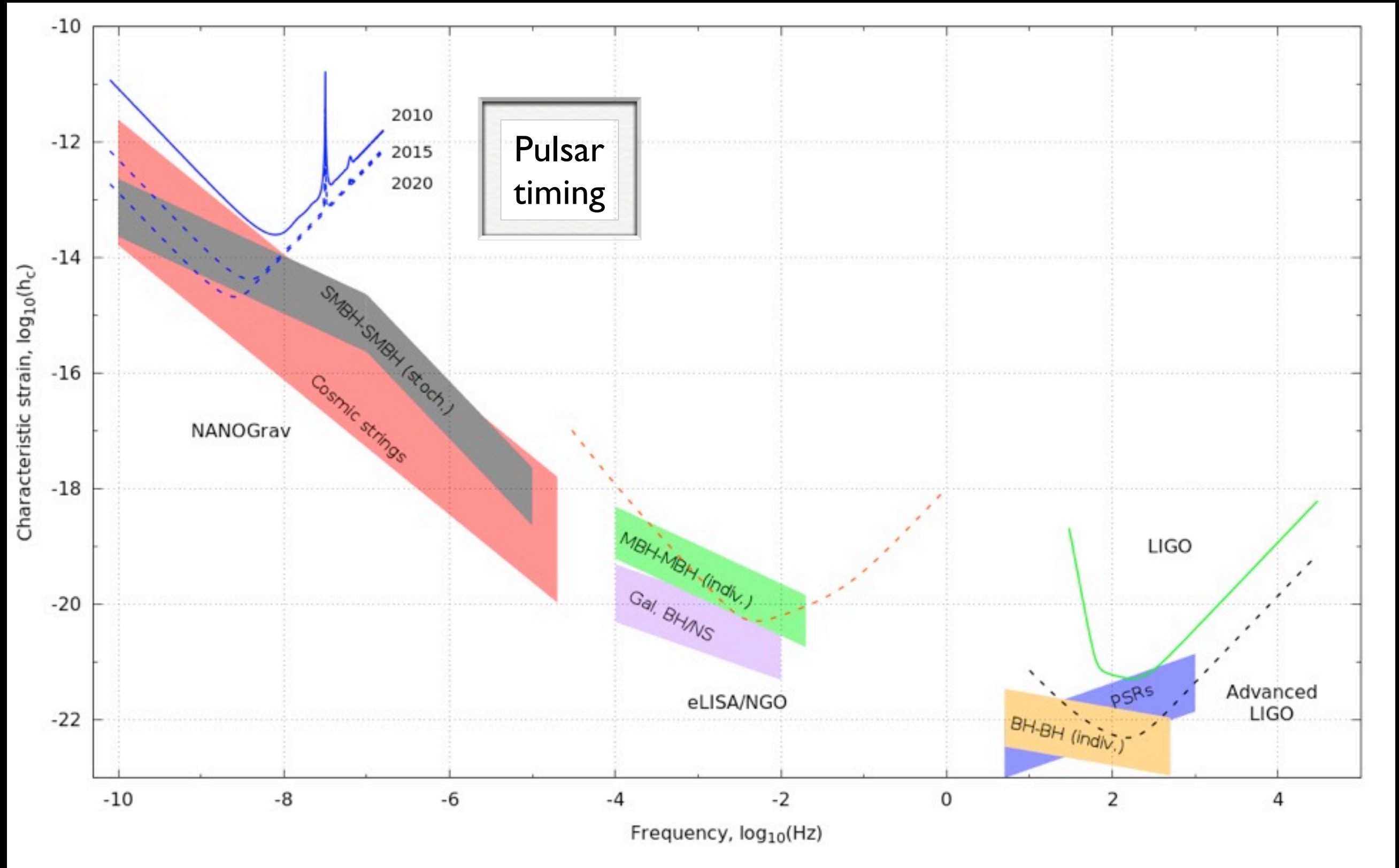
Draft version April 3, 2015

ABSTRACT

ning of one of the most precise pulsars: PSR J1713+0747. The pulsar's pulse profile was modeled, with residuals having weighted root mean square of ~ 92 ns, by a complex model that includes the mass and three-dimensional orbit of its white dwarf companion and includes short- and long-timescale correlated noise such as jitter and red noise. The new measurements greatly improve previous measurements of the system properties, including the masses of the pulsar ($1.31 \pm 0.11 M_{\odot}$) and white dwarf ($0.286 \pm 0.012 M_{\odot}$) as well as their parallaxes. We measured a change in the observed orbital period of PSR J1713+0747, which we interpret as a change in the orientation of the binary system and the Earth. The intrinsic change in orbital period is not distinguishable from zero. This result, combined with the measured P_b^{Int} , provides constraints on potential changes in the gravitational constant G as predicted in some theories of gravity. We found that \dot{G}/G is consistent with zero [$(-0.6 \pm 1.1) \times 10^{-12} \text{ yr}^{-1}$, 95% confidence level], at least a factor of 31 (99.7% confidence level) more slowly than the average rate of expansion of the universe. This is the best \dot{G}/G limit from pulsar binary systems. The P_b^{Int} of pulsar J1713+0747 is consistent with the prediction of general relativity based on the putative coupling constant for dipole gravitational radiation κ_D . We find $\kappa_D = (-0.9 \pm 3.3) \times 10^{-4}$, consistent with zero. Finally, the nearly circular orbit of the pulsar allows us to constrain statistically strong-field post-Newtonian parameters Δ , which describes the equivalence principle, and $\hat{\alpha}_3$, which describes a breaking of both Lorentz invariance and conservation of momentum. We found at 95% confidence level $\Delta < 0.01$ and $\hat{\alpha}_3 < -0.0747$.



Predicted Power in Gravitational Radiation



VLBI Resolution of the Pleiades distance controversy

Melis et al. (2014)

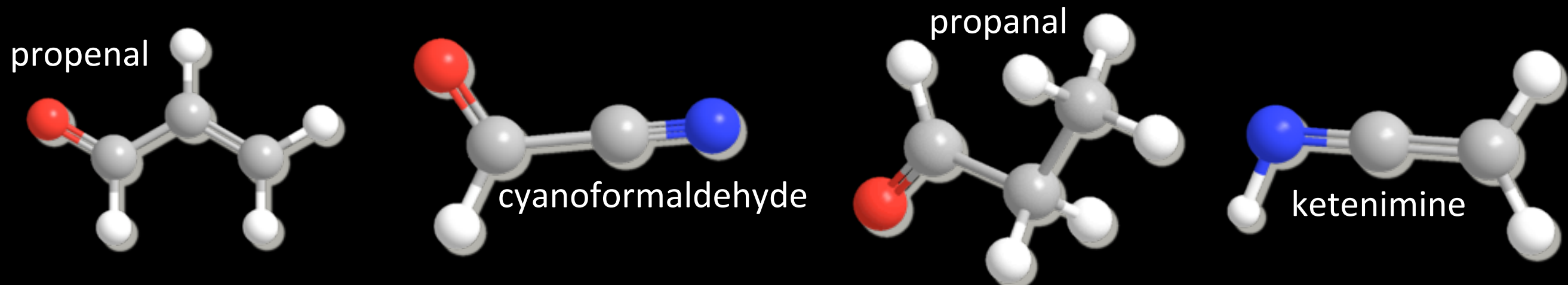


The Chemistry of Interstellar Space

Some (of the 17+) New GBT Molecule Detections



The Chemistry of Interstellar Space

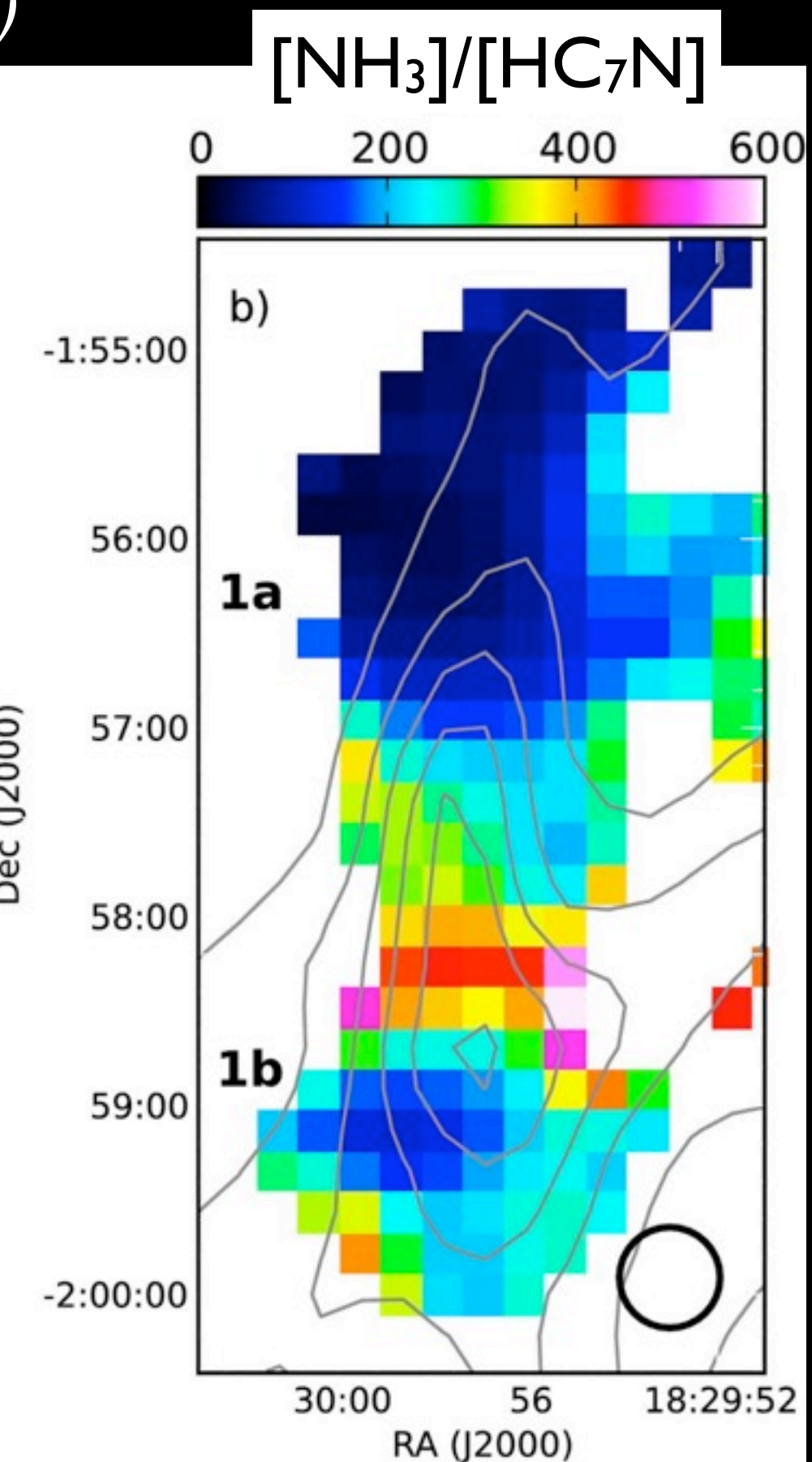
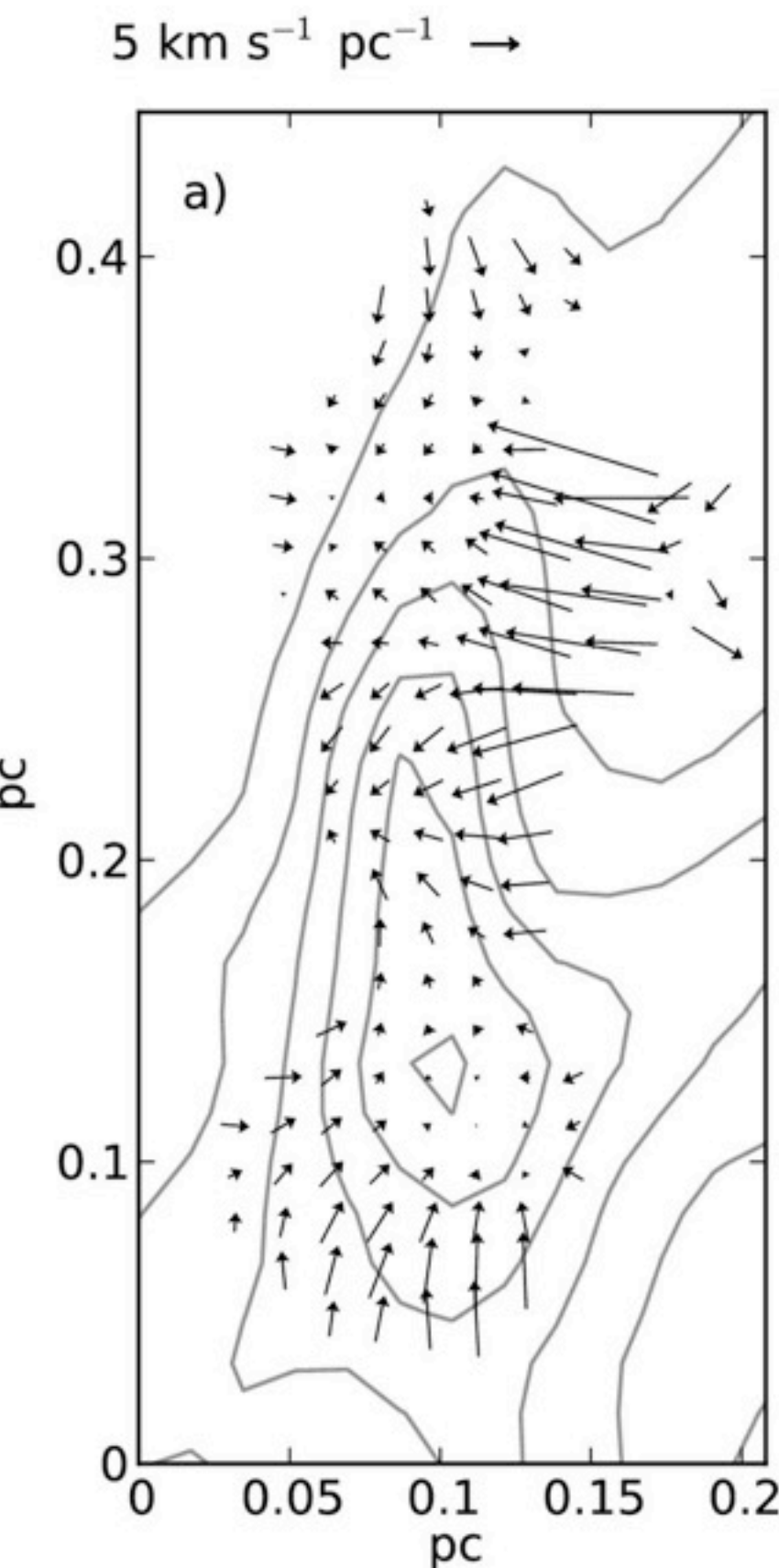
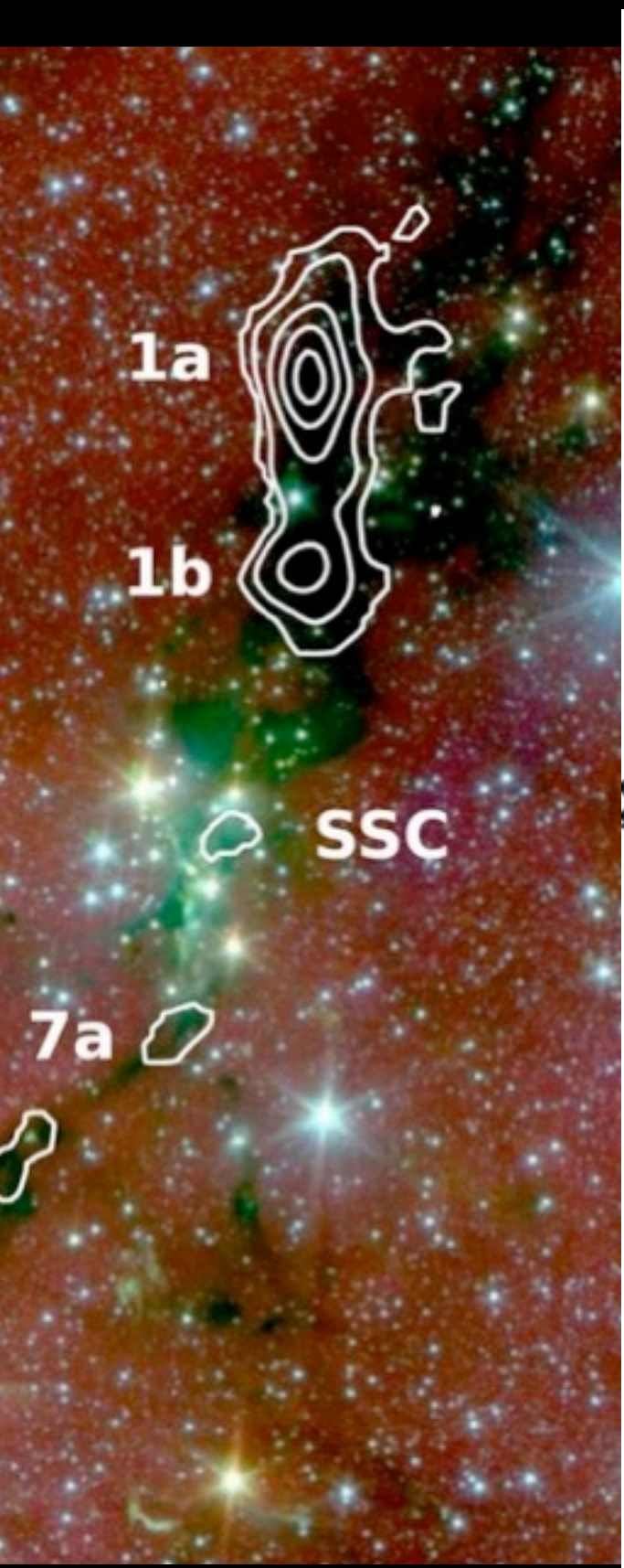


Some (of the 17+) New GBT Molecule Detections

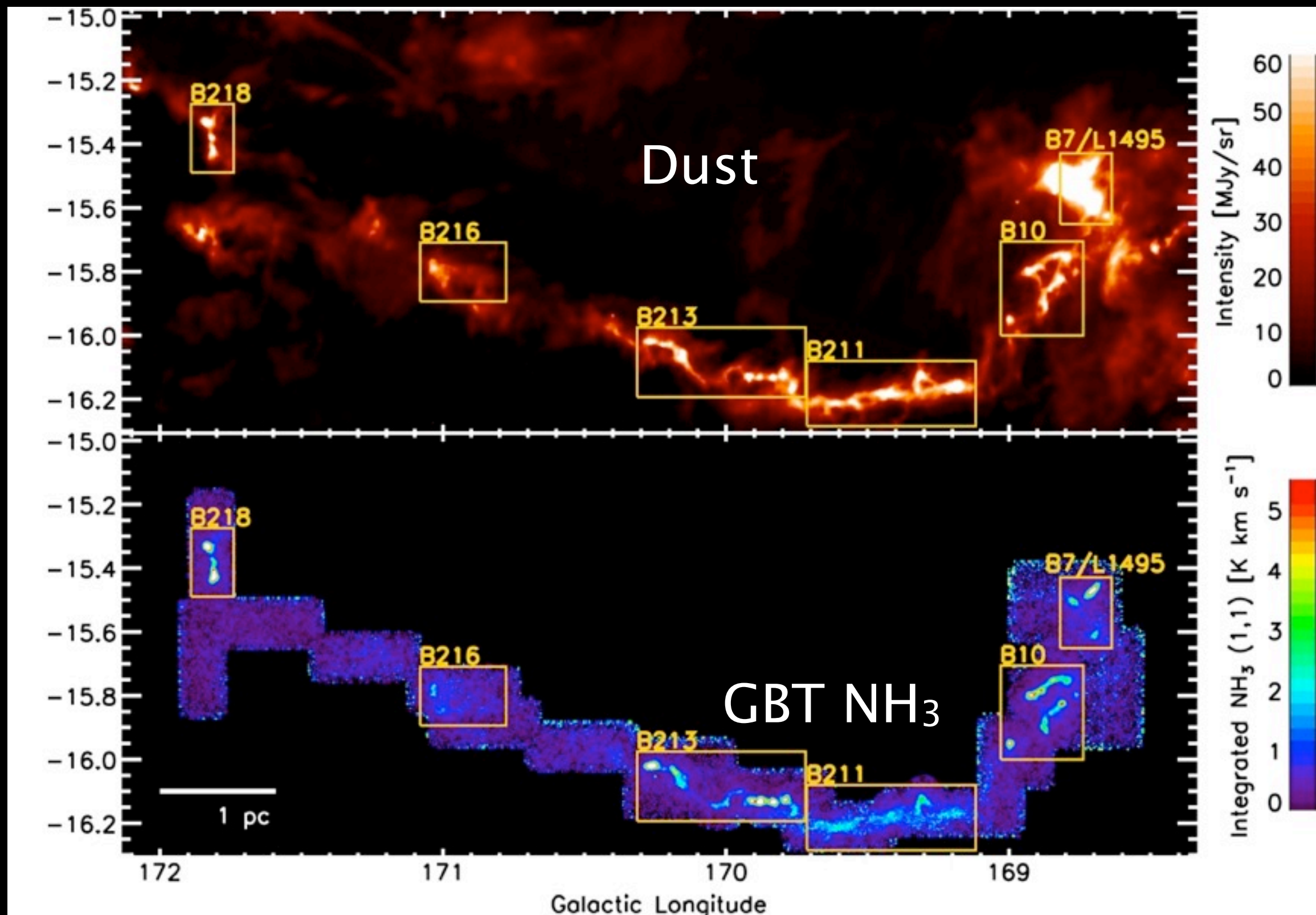


HC_7N : A Chemical “Clock” in a Molecular Cloud?

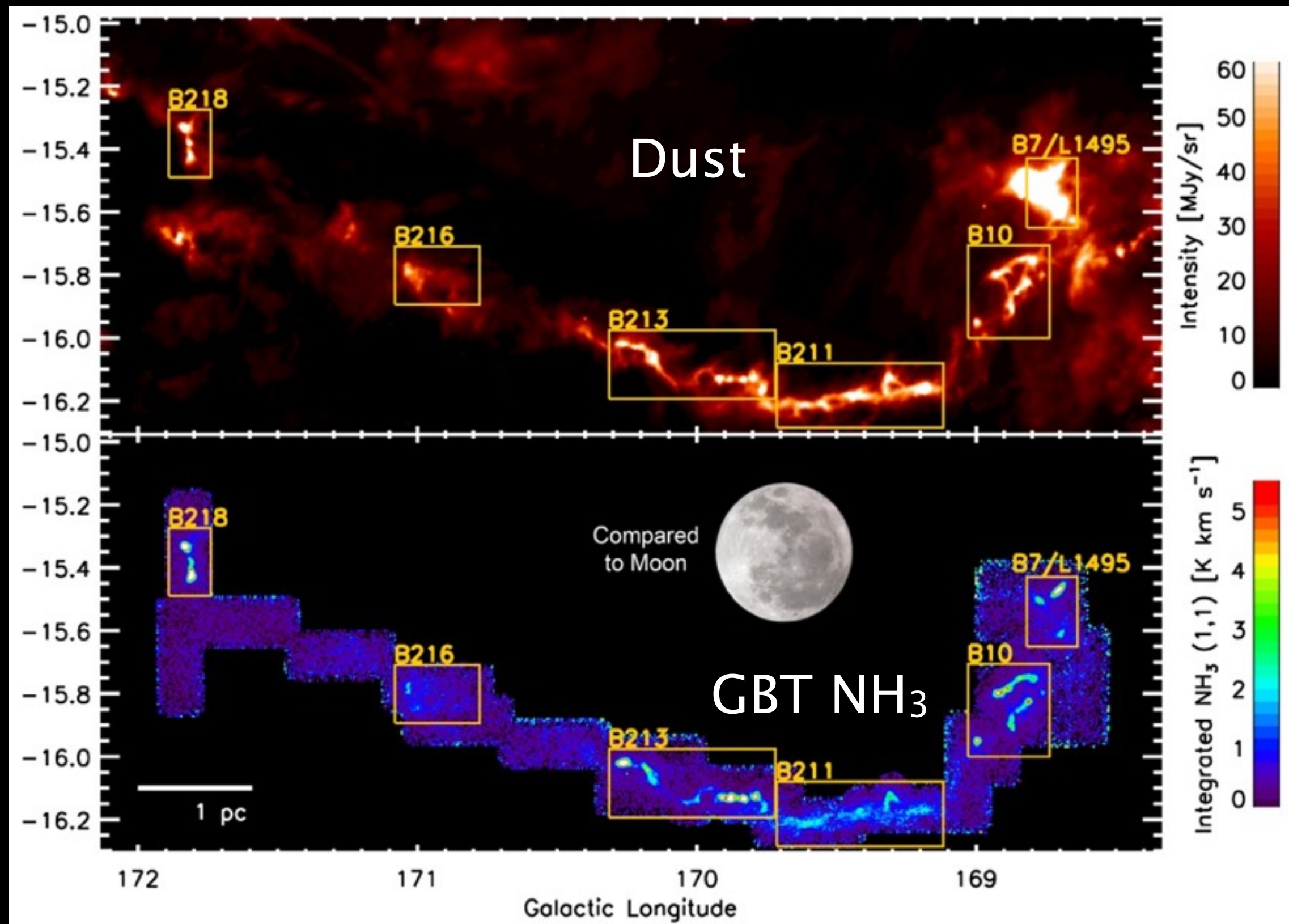
Friesen et al. (2013)



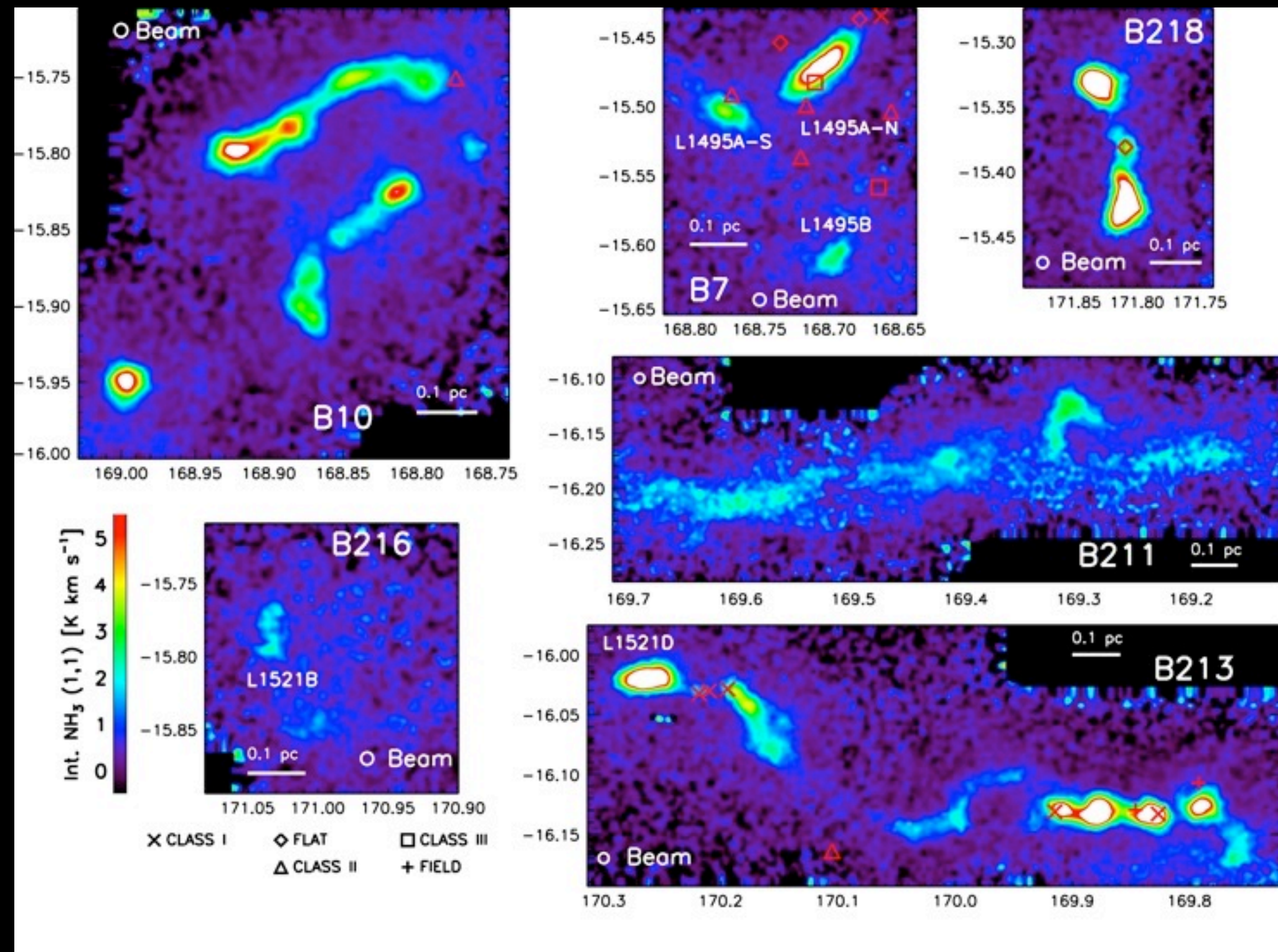
Star Formation in a Filament in Taurus



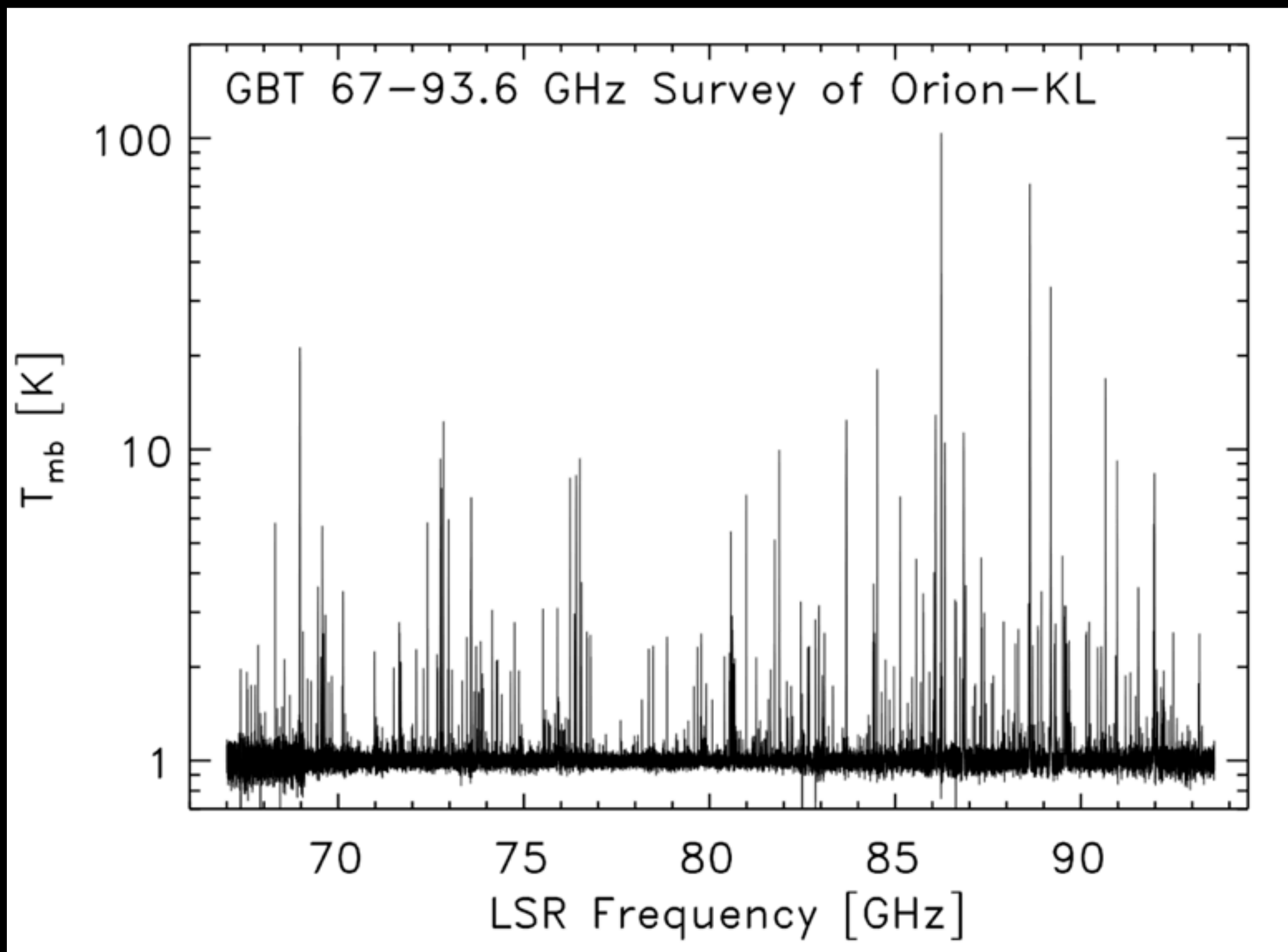
Star Formation in a Filament in Taurus



Star Formation in a Filament in Taurus



GBT W-band Spectral Survey



Frayer et al. (2015)

GBT detection of mm-cm sized “dust” in star-forming clouds



5'



Schnee et al. (2014)

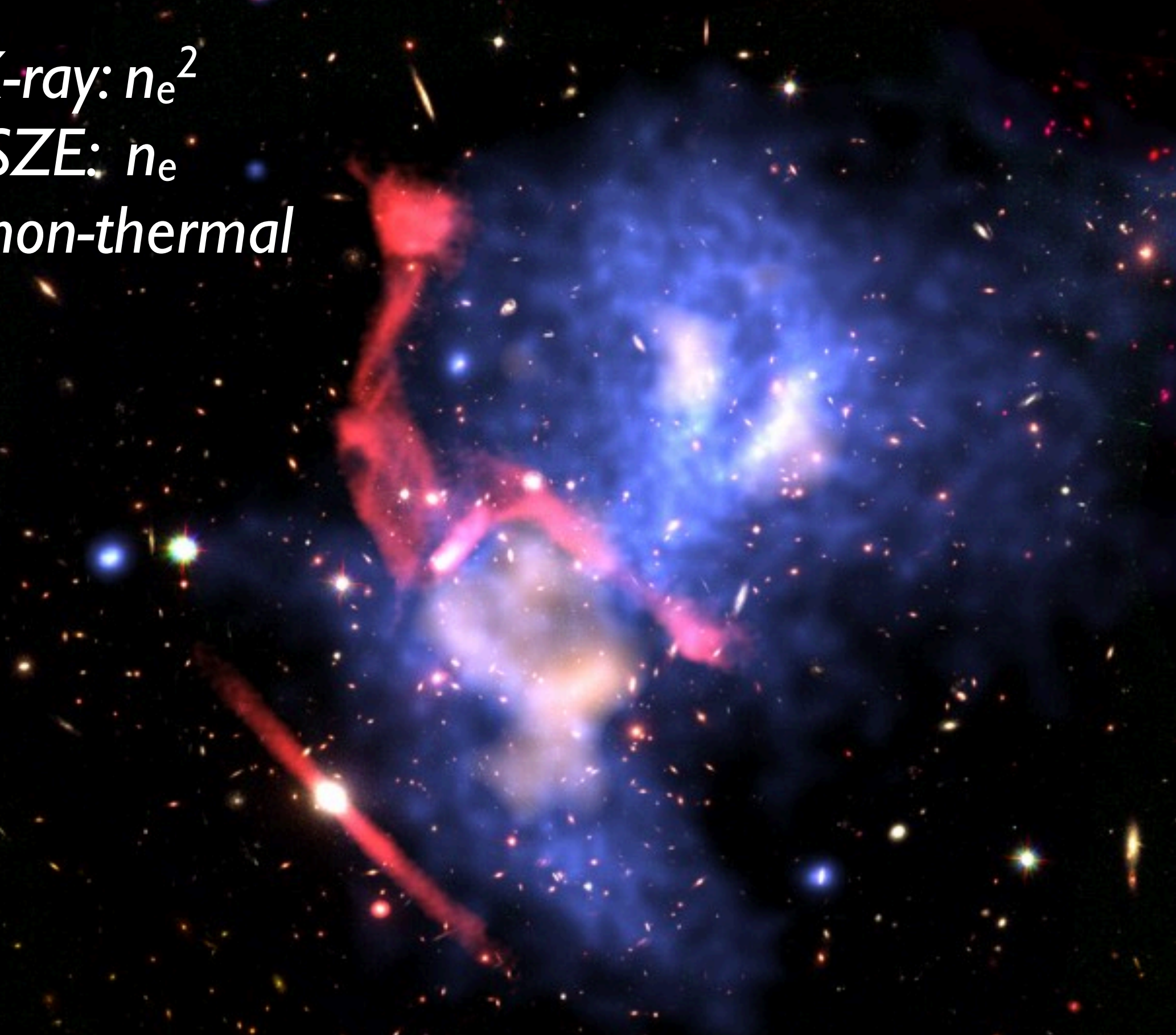
MUSTANG
Bolometer Array
3.3mm
81–96 GHz

GBT High-Resolution SZE in a Galaxy Cluster

X-ray: n_e^2

SZE: n_e

VLA non-thermal



HI “Intensity Mapping”

Ui-Le Pen, Jeffrey B. Peterson et al.

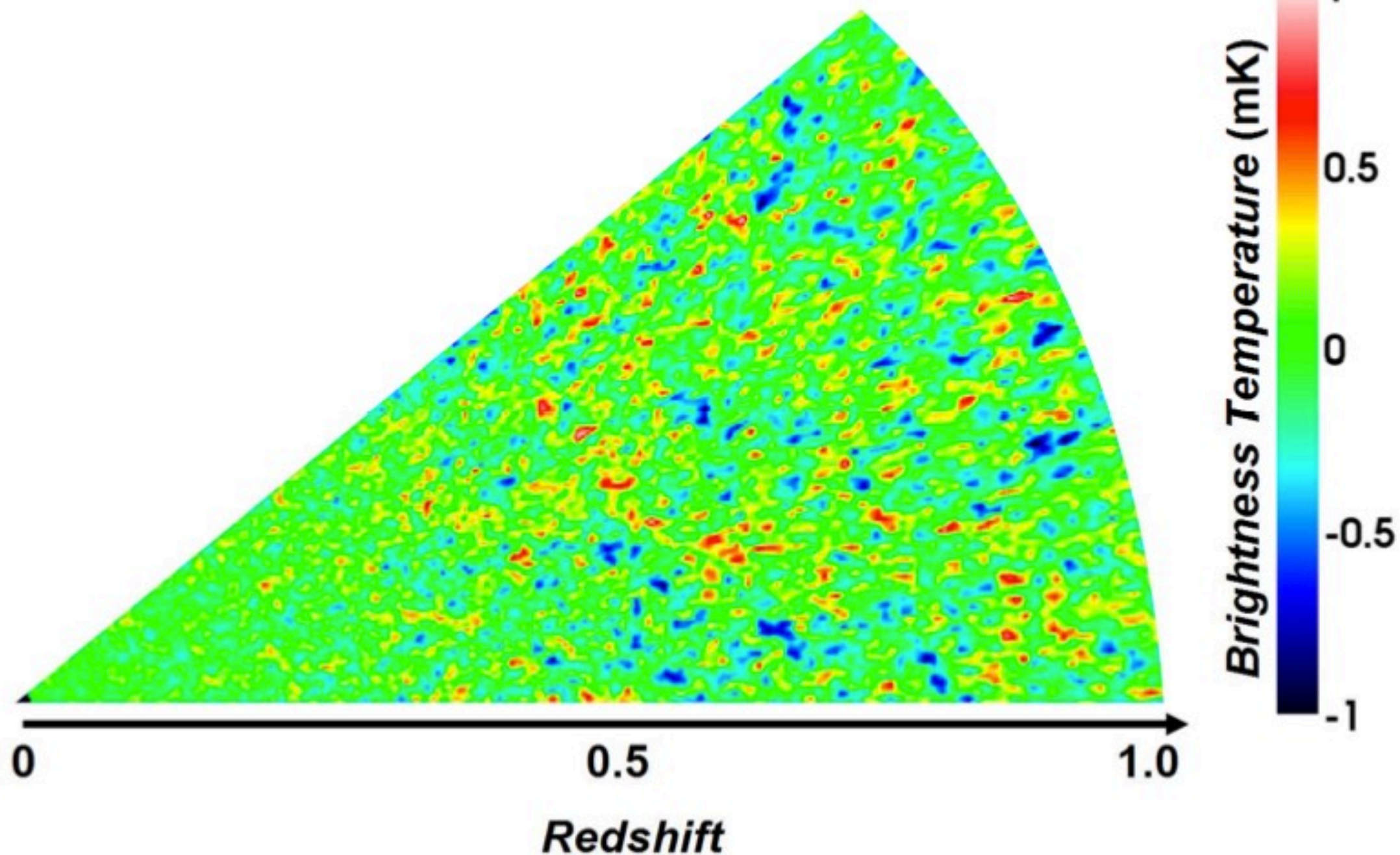
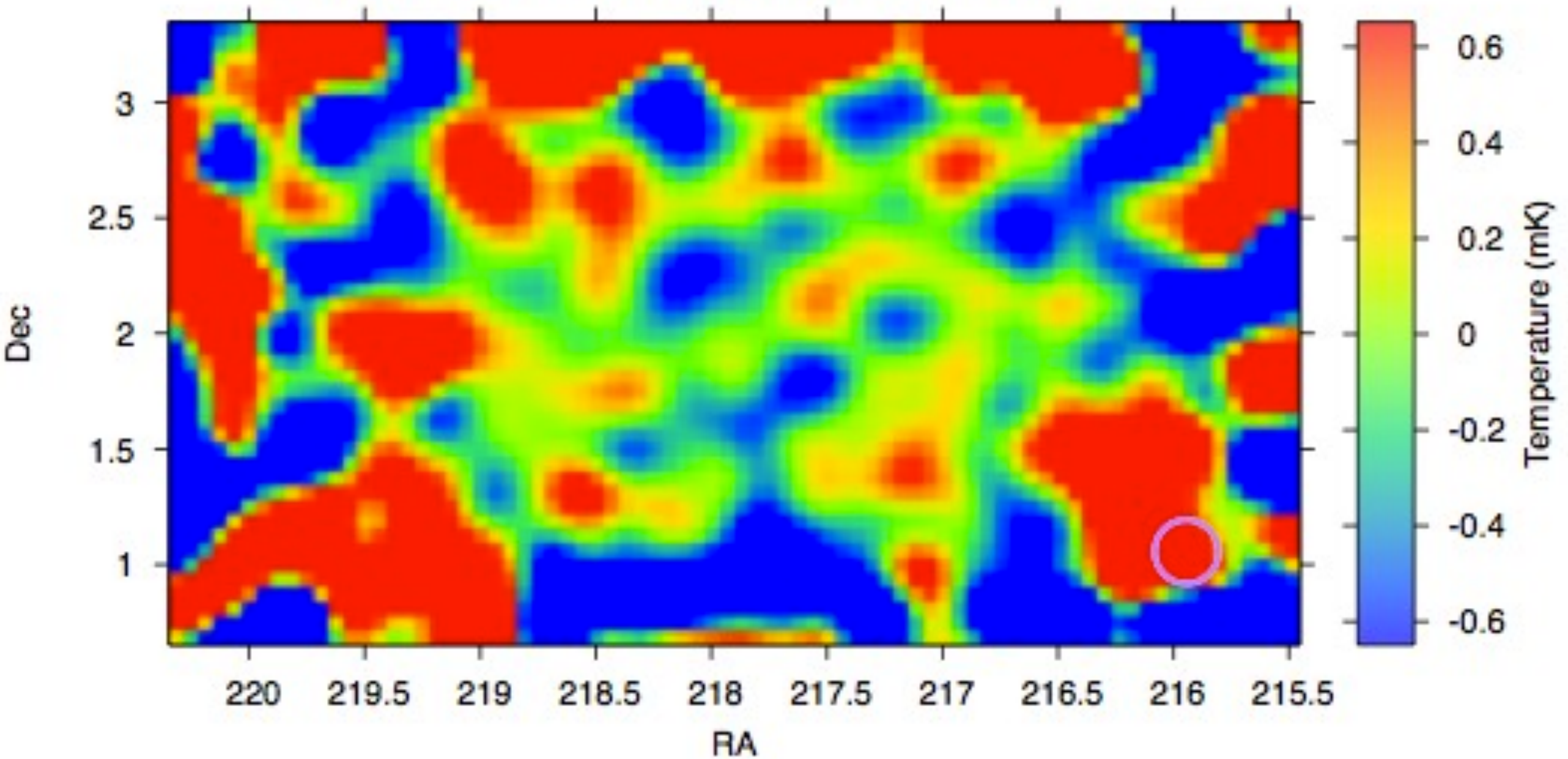


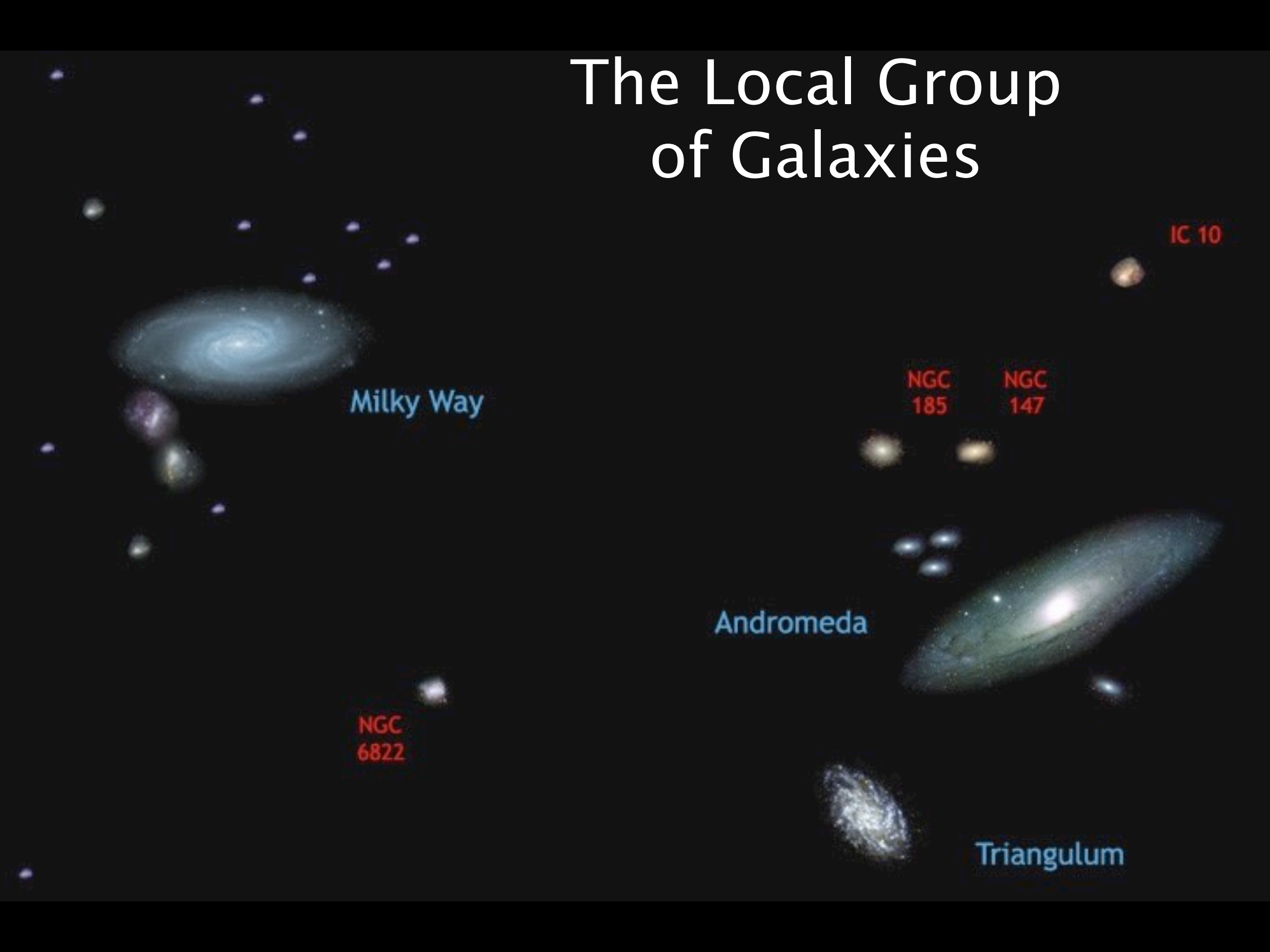
Figure 2: Simulated fluctuations in the brightness temperature of 21cm emission from galaxies in a slice through the universe. The emission is smoothed over $8/h$ Mpc. The redshift, z , translates to frequency: $\nu = 1.42\text{GHz}/(1+z)$. Red indicates overdensity and blue underdensity.

GBT 15hr field, cleaned, beam convolved (800.4 MHz, $z = 0.775$)



Masui et al. (2013)

The Local Group of Galaxies



No Hydrogen in the Milky Way's Dwarf Galaxies



Galaxy	L (L_\odot)	M_{HI} (M_\odot)
Segue I	340	<11
UMa II	41,000	<74
Bootes II	1,000	<38
Coma Ber	3,700	<62
Ursa Mi	280,000	<63
Draco	280,000	<133
Spitzer Cloud		400

GBT results from Spekkens et al. 2014

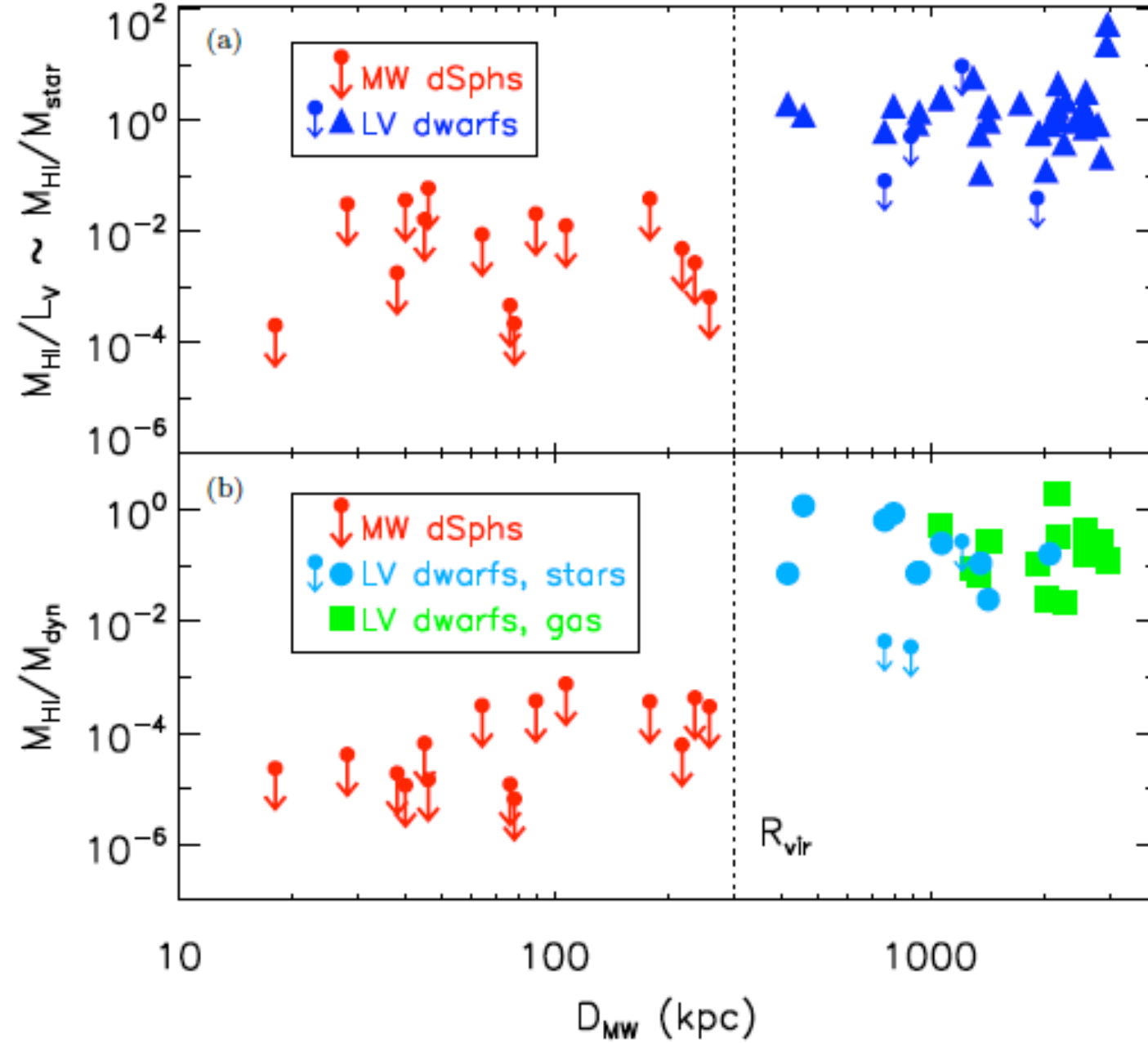
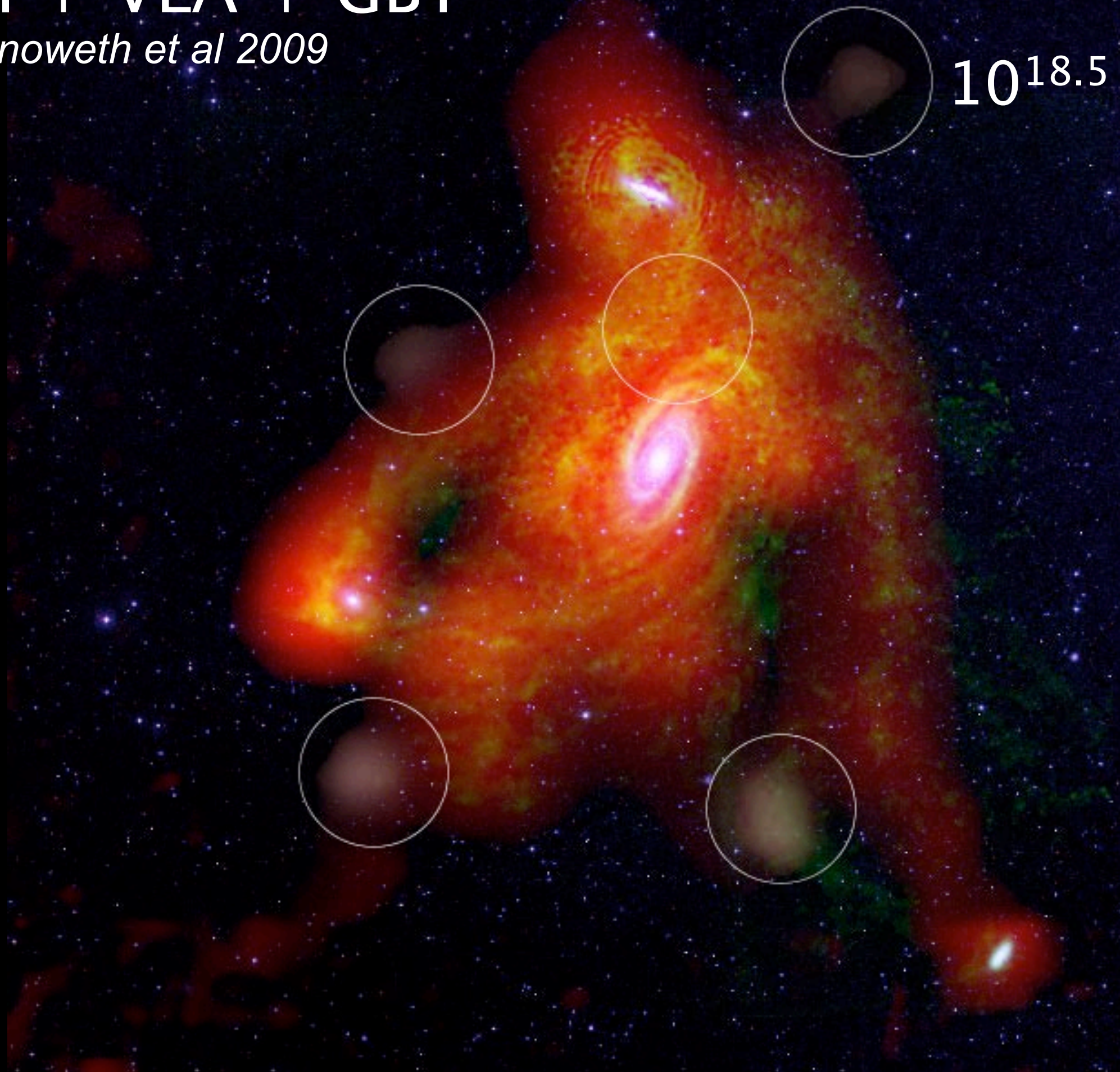


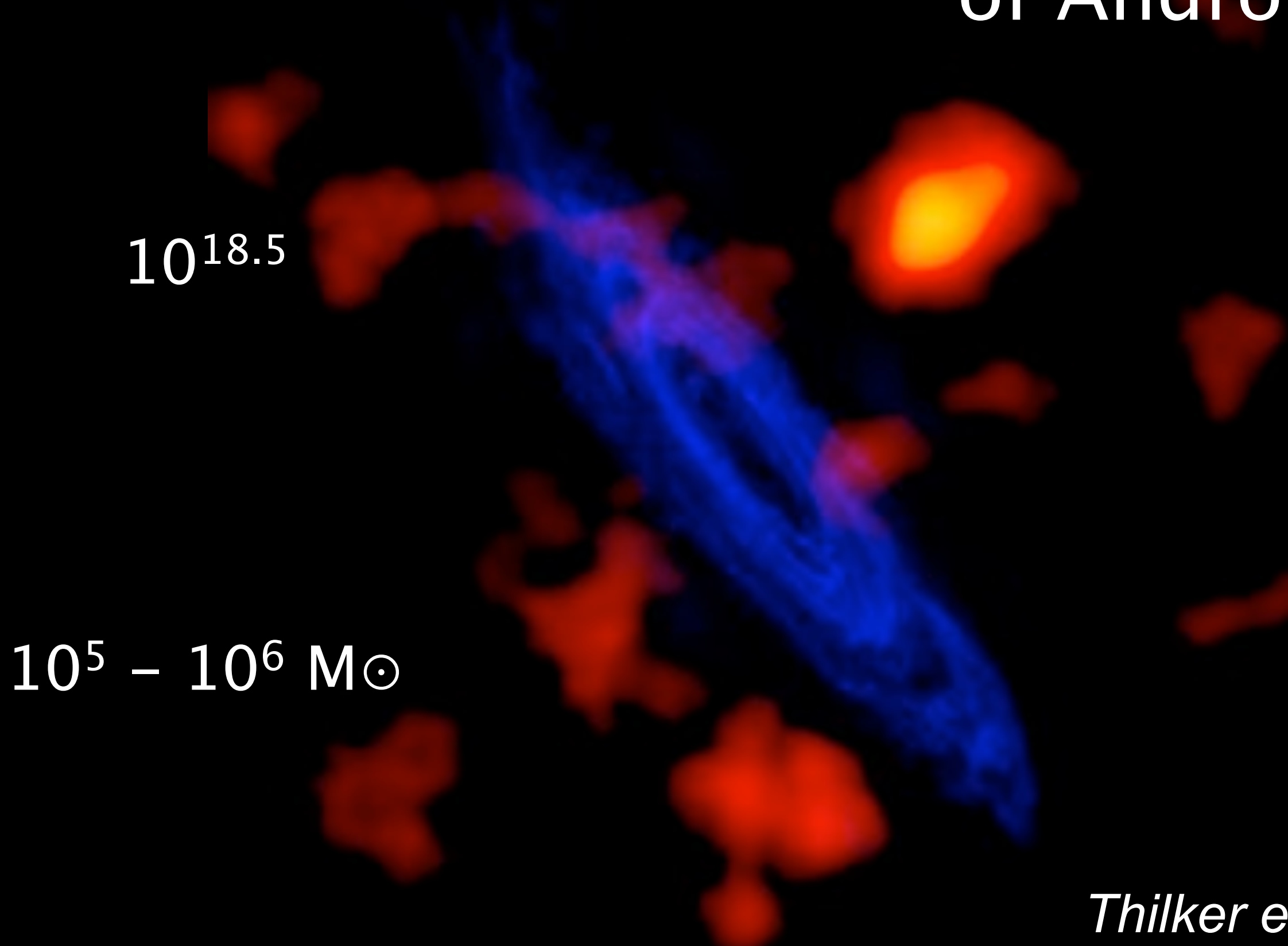
Figure 2. H_1 content of the Milky Way dSphs and Local Volume dwarfs, normalized by (a) V-band luminosity L_V (\sim the stellar mass M_*), and (b) dynamical mass M_{dyn} . In panel (a), the red arrows show $M_{\text{H}_1}^{\text{lim}}/L_V$ for the sample Milky Way dSphs, and the blue filled triangles and arrows show M_{H_1}/L_V and $M_{\text{H}_1}^{\text{lim}}/L_V$, respectively, for systems classified as Local Group satellites or nearby neighbors by M12. In panel (b), the red arrows show $M_{\text{H}_1}^{\text{lim}}/M_{\text{dyn}}$ for the sample Milky Way dSphs, where M_{dyn} is computed from stellar kinematics. The light blue filled circles and arrows show $M_{\text{H}_1}/M_{\text{dyn}}$ and $M_{\text{H}_1}^{\text{lim}}/M_{\text{dyn}}$ for Local Volume satellites, respectively, where M_{dyn} is computed from stellar kinematics. The green filled squares show $M_{\text{H}_1}/M_{\text{dyn}}$ for Local Volume satellites where gas kinematics are used to compute M_{dyn} . The vertical dotted line in both panels shows the approximate virial radius of the Milky Way, $R_{\text{vir}} = 300$ kpc.

Optical + VLA + GBT

Chynoweth et al 2009



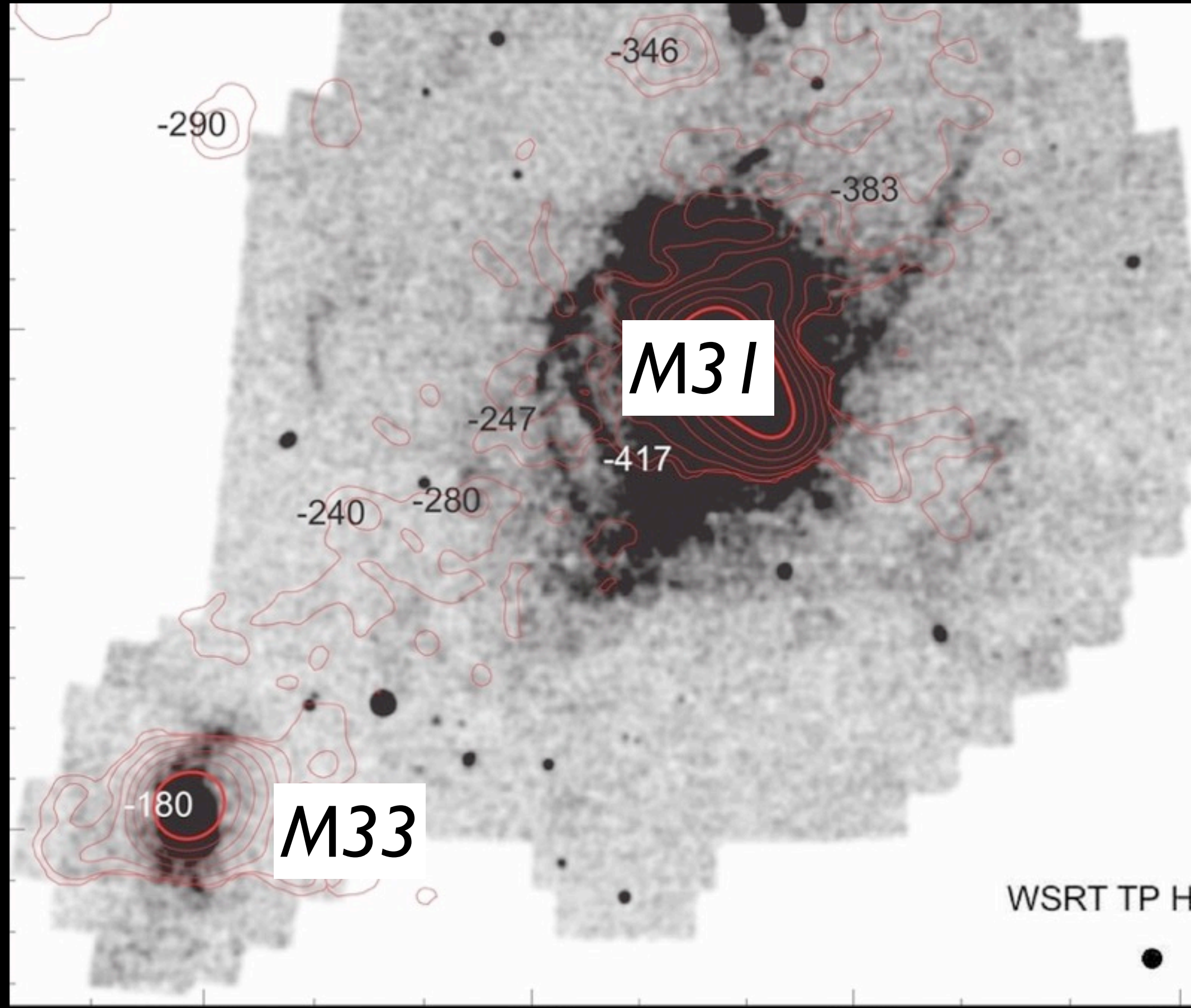
GBT HI study of Andromeda

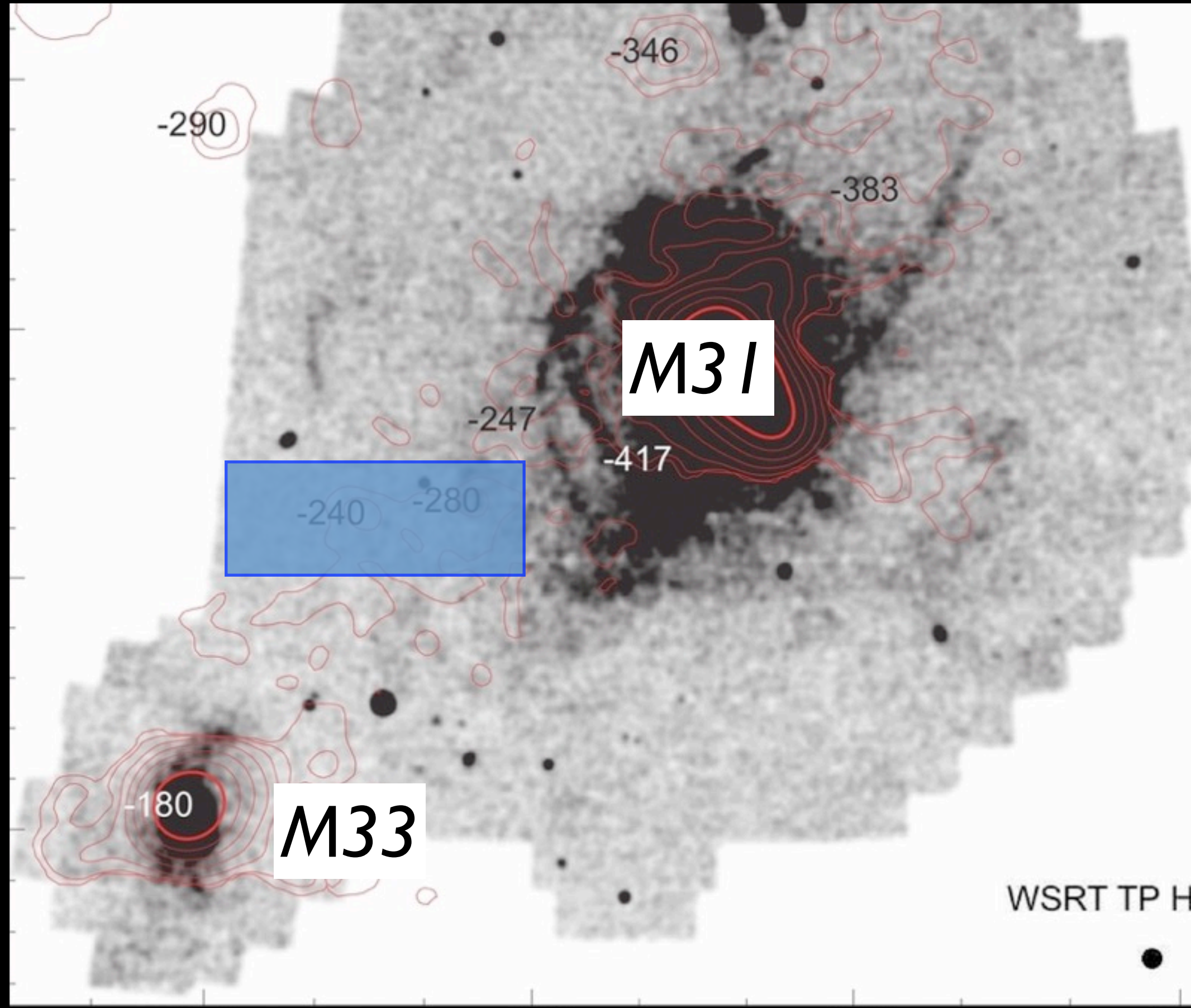


Thilker et al 2004

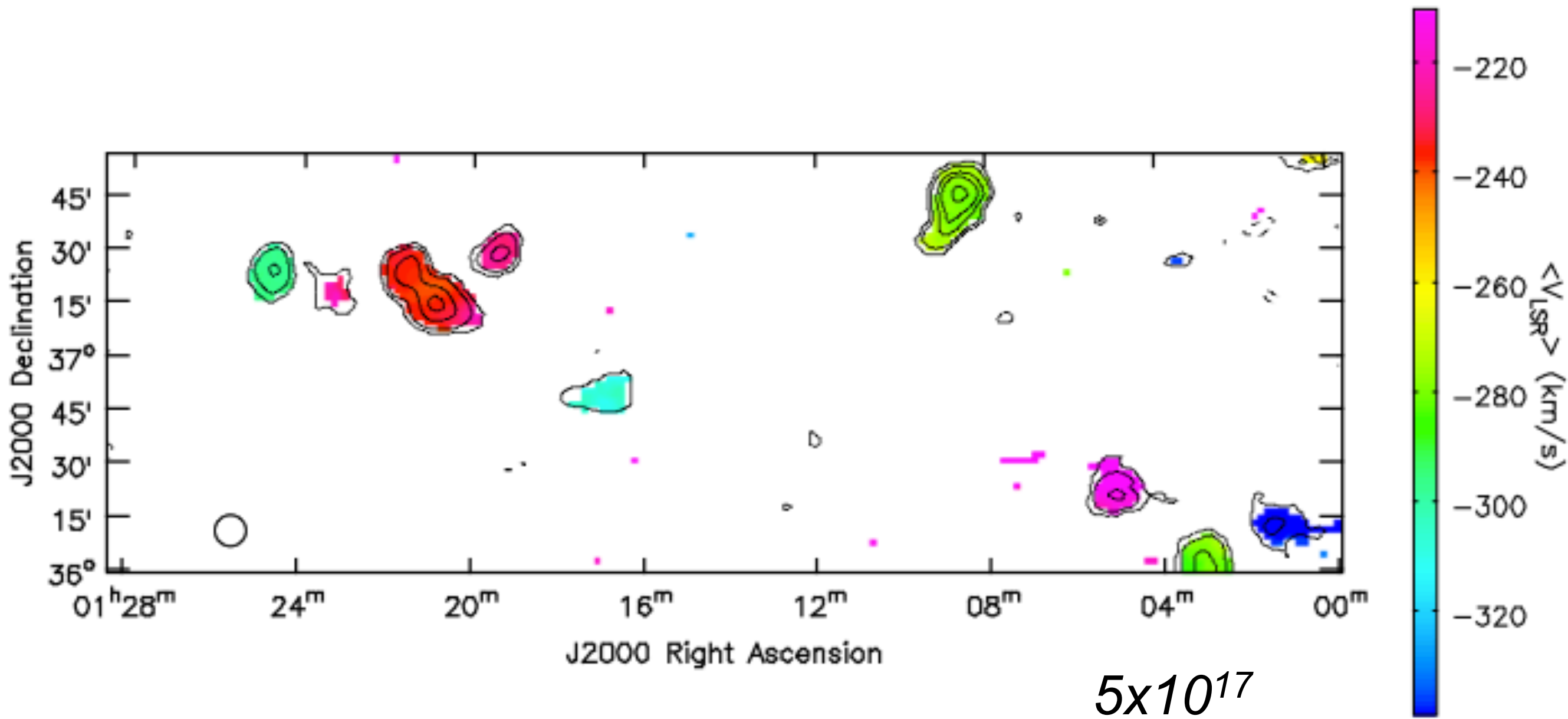
Andromeda is
devouring its
smaller neighbors





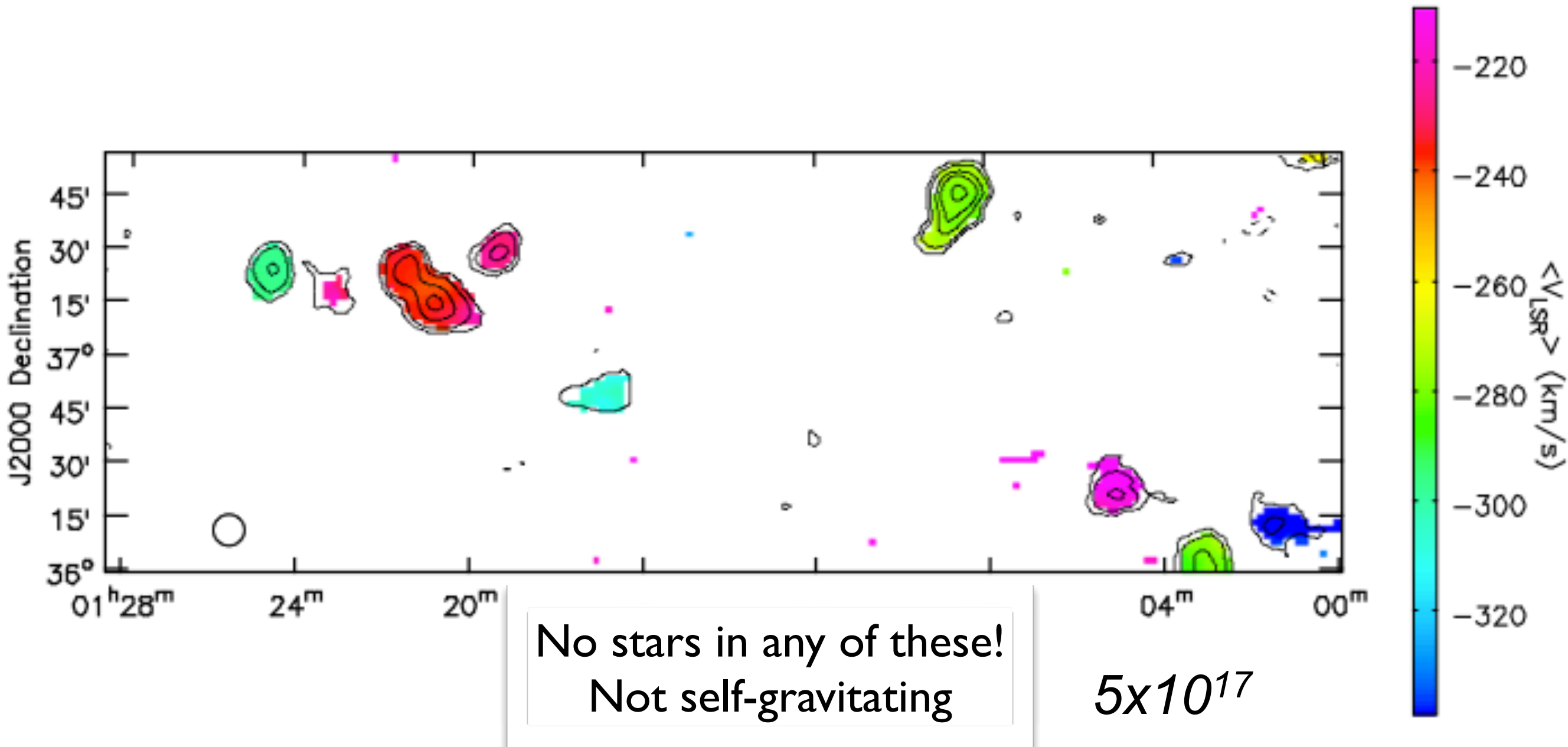


GBT detection of Local Group Gas Clouds

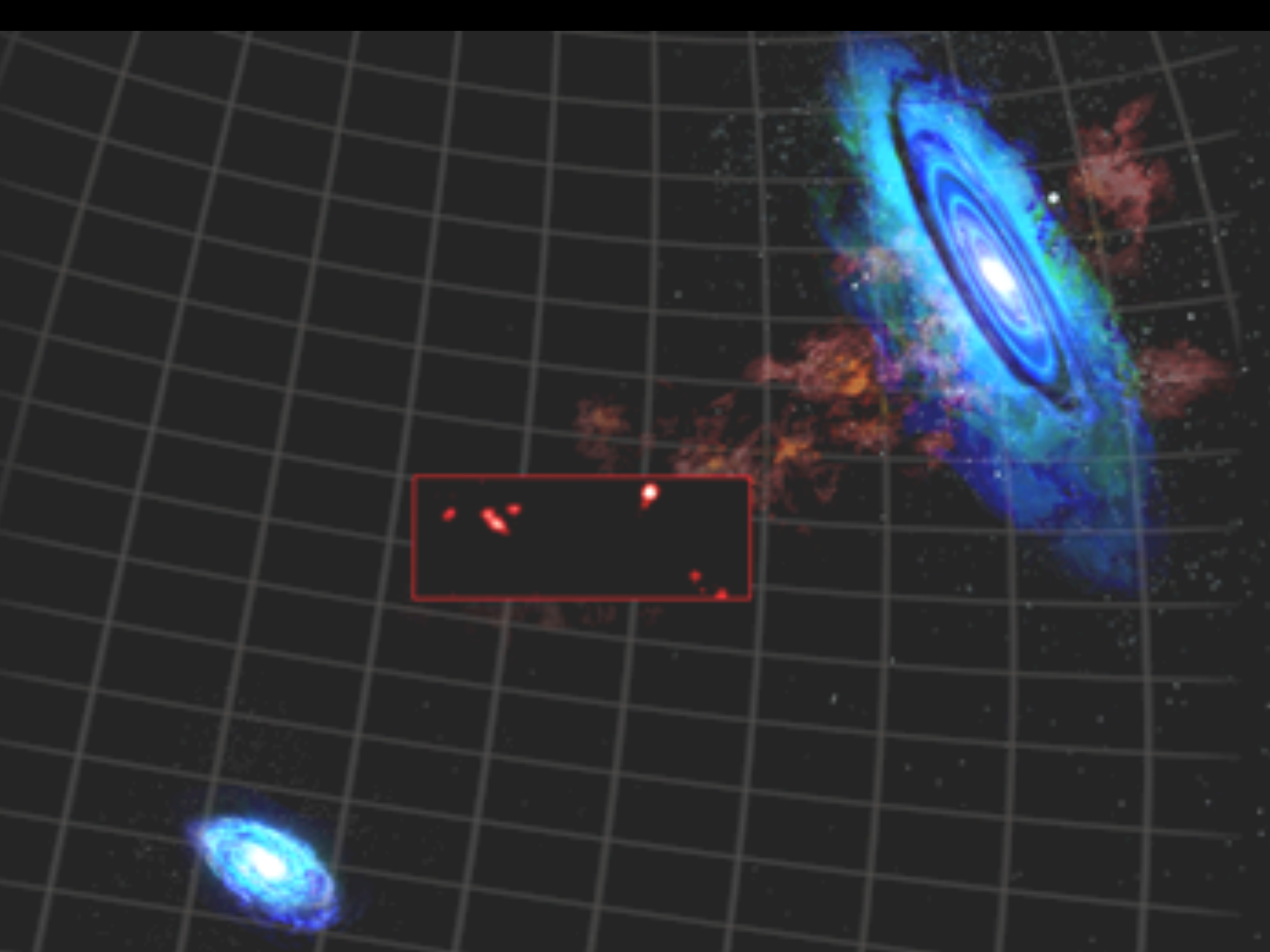


Wolfe et al. 2013
Wolfe, Lockman, & Pisano 2015

GBT detection of Local Group Gas Clouds



Wolfe et al. 2013
Wolfe, Lockman, & Pisano 2015



The GBT in 2016+



The GBT in 2016+

VEGAS

(NSF grant to UC Berkeley)

- 16 spectrometers
- Up to 8 spectral windows per spectrometer
- Up to 1.25 GHz per spectrometer



ARGUS -- 8" GBT spectroscopy at 3mm

6 0

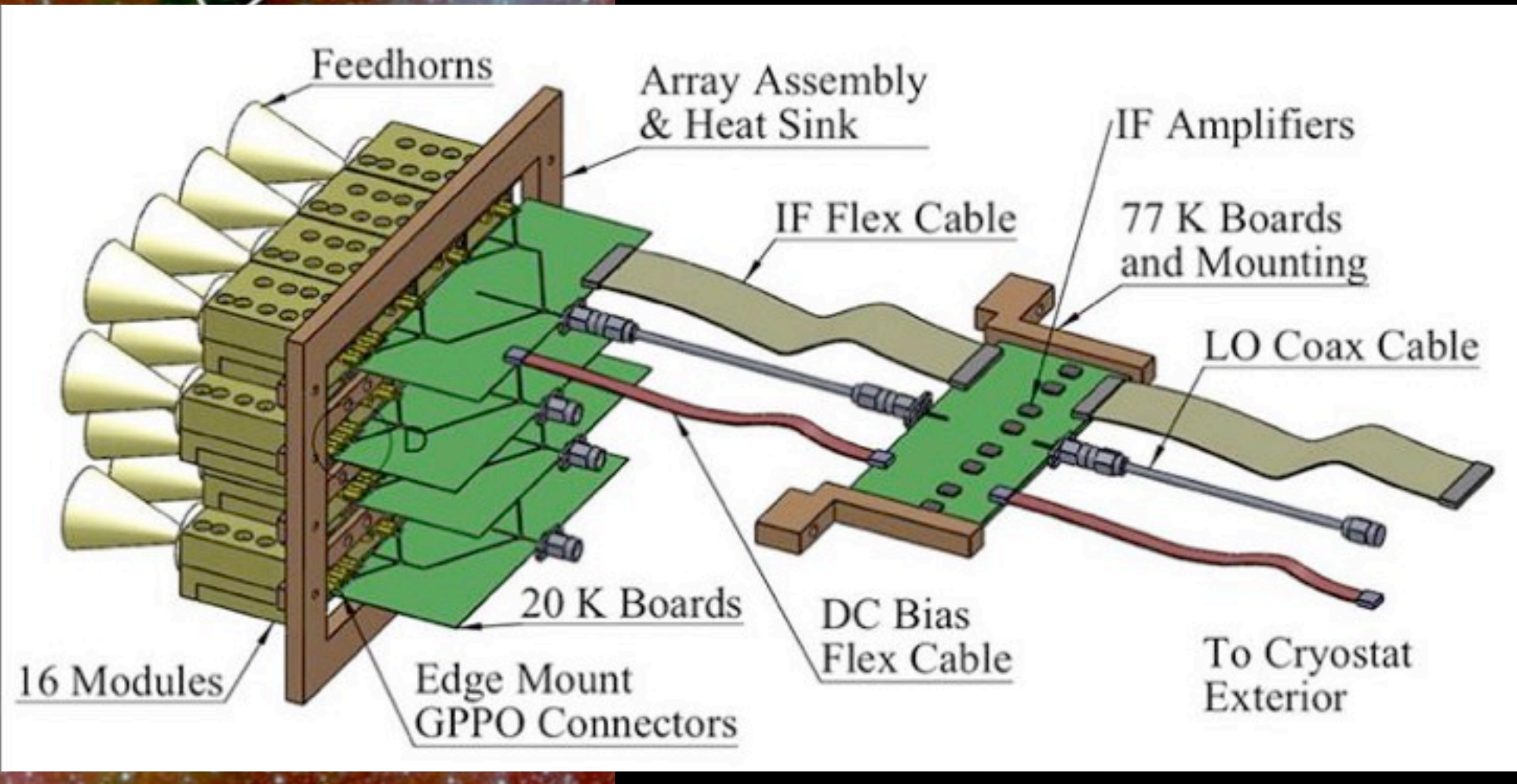
1a

1b

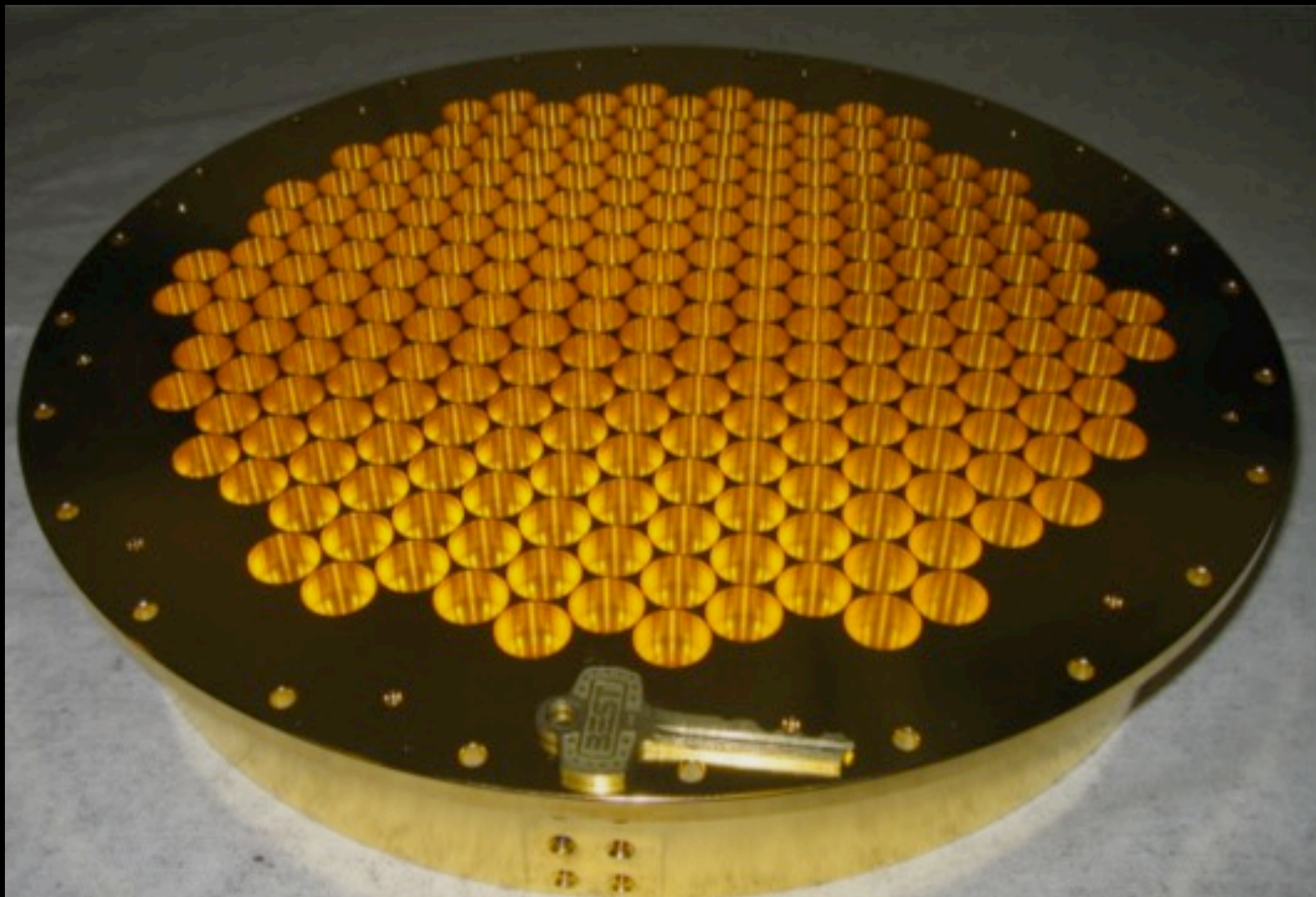
7
7b



- 16 element scalable 75-115 GHz FPA
- Stanford/CIT-JPL/UMd/Miami/NRAO (NSF grant to Stanford)



GBT MUSTANG - 2 (*NSF grant to Univ Penn*)

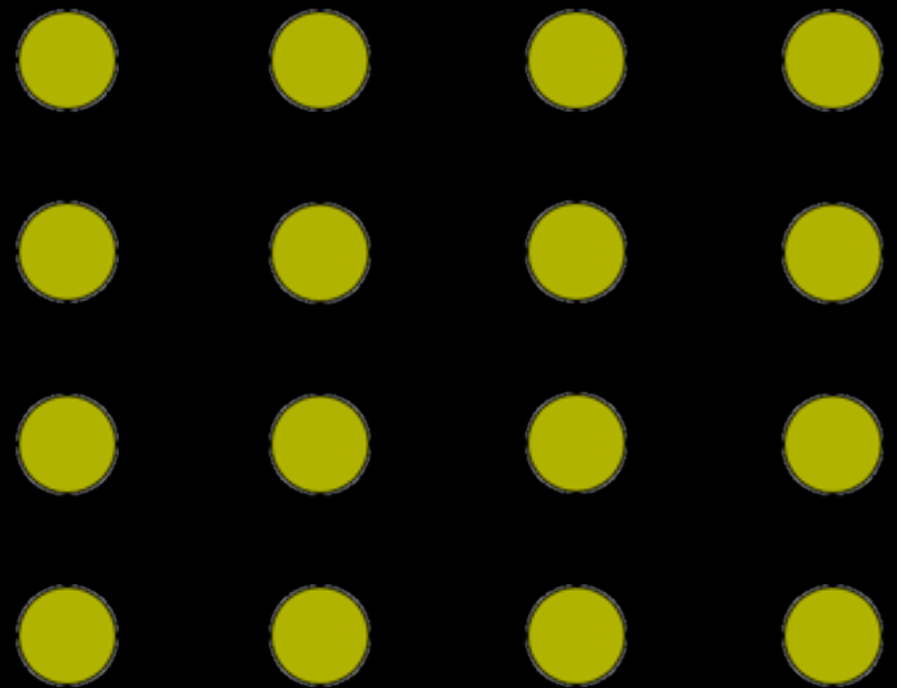


223 pixels
>4' FOV
35x faster than MUSTANG

ARGUS 3mm 16-pixel camera



footprint



\approx 4% complete sampling

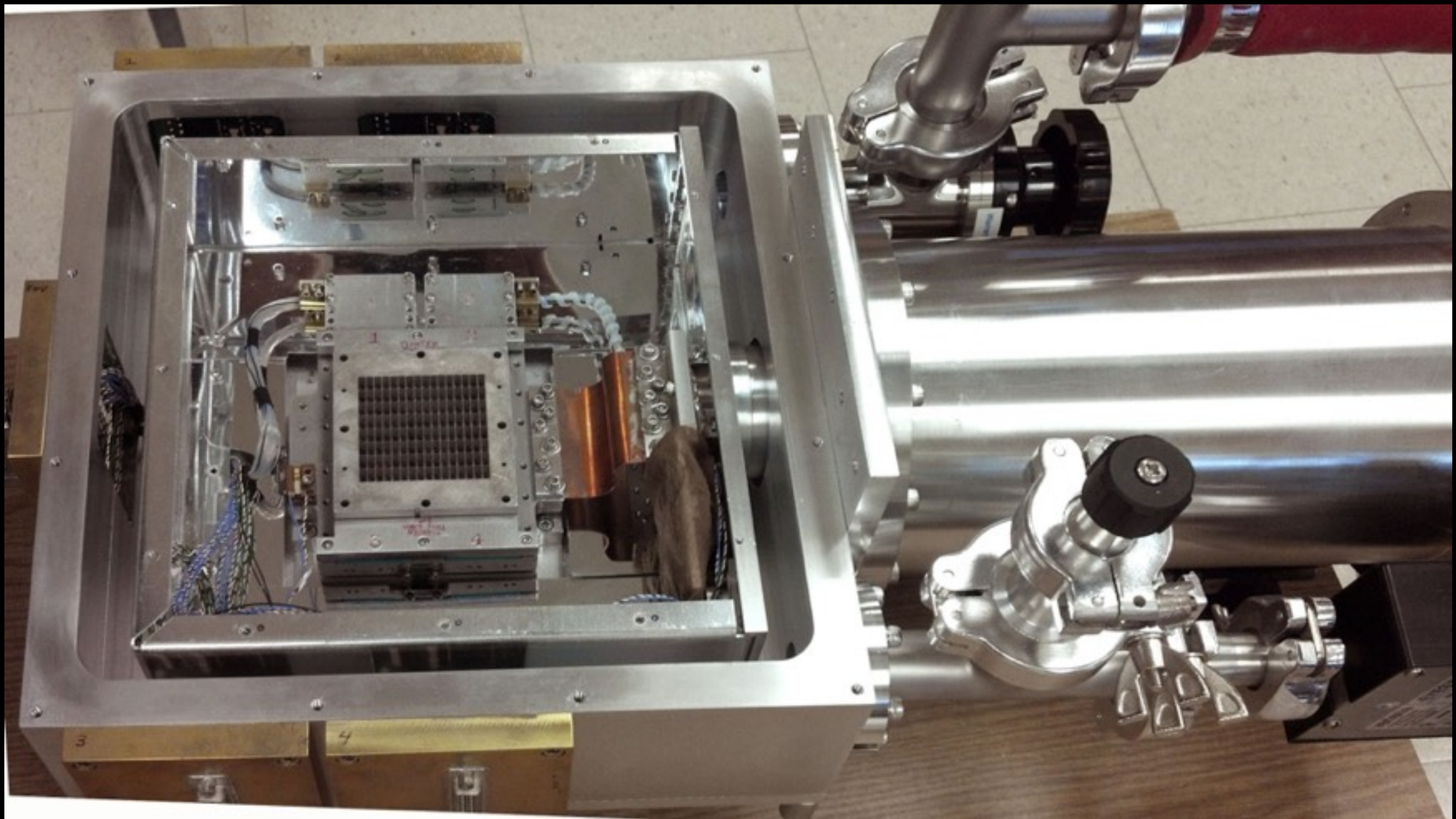
FLAG 21cm



UMass Scalable 75-115 GHz PAF

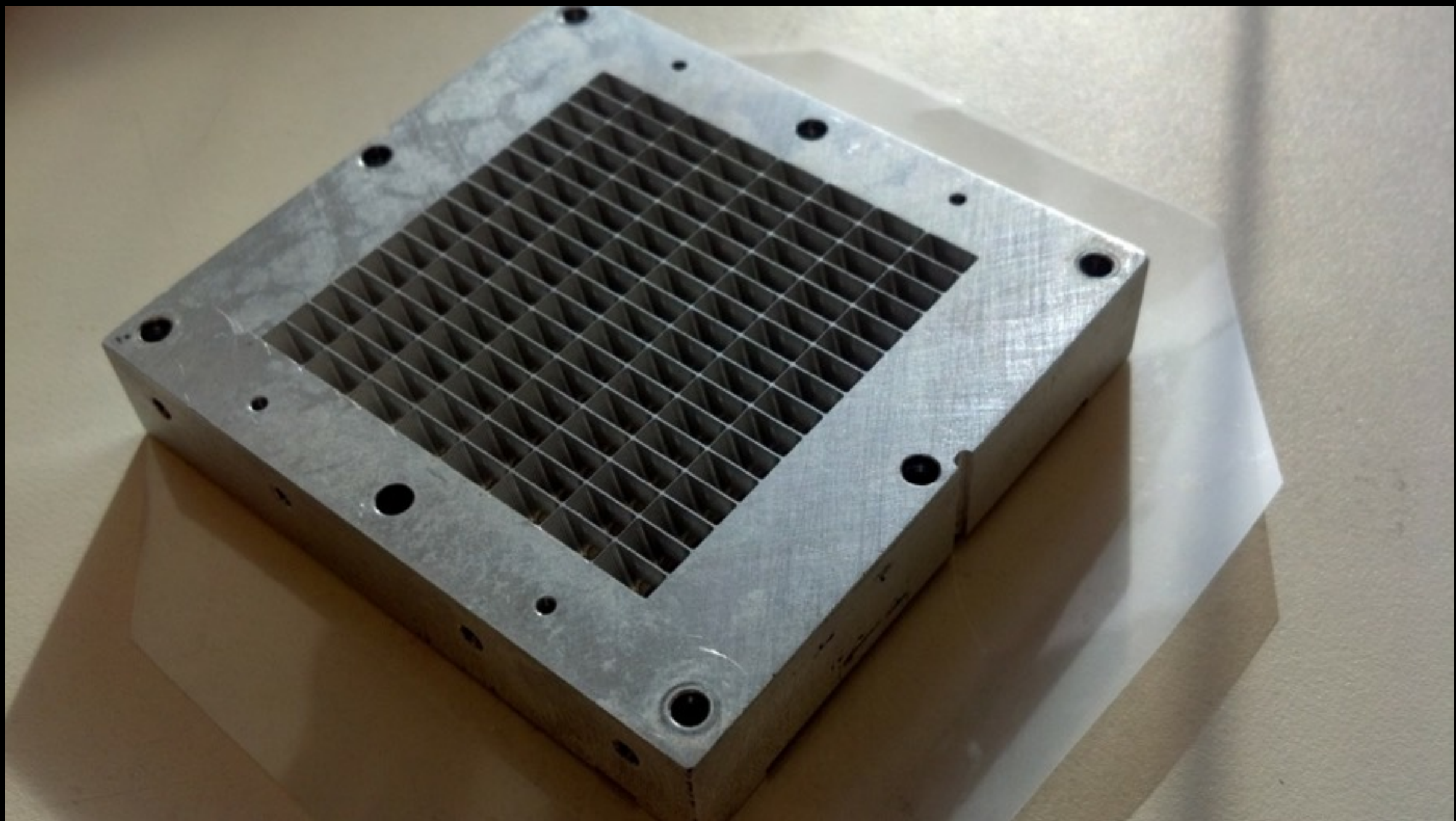
The wave of the future

UMass Scalable 75-115 GHz PAF



The wave of the future

UMass Scalable 75-115 GHz PAF





How do I get to use the GBT?

